Inclusion behaviour of related organic host compounds

by

NOBATHEMBU FALENI

A thesis submitted to the Cape Peninsula University of Technology
in fulfilment of the requirements for the

MASTERS DEGREE IN TECHNOLOGY
(CHEMISTRY)

Department of Chemistry

August 2007

Acknowledgements

I would like to thank:

- My Supervisor, Dr Ayesha Jacobs for assisting me throughout my research.

- My family and friends for their support.

- My Supernatural Dad, for His abundant Grace, Mercy and I give Him All the Glory.

Publication and conference

Parts of this thesis have been published:

Inclusion by a Xanthenol Host: Relating Structure to the Kinetics of Desolvation and Guest Exchange, A. Jacobs; N. Faleni; L. R. Nassimbeni and J.H. Taljaard, *Crystal Growth and Design* 2007, Vol. 7, 6, 1003-1006.

Parts of this thesis have been presented at the following conference:

- Poster entitled: Inclusion behaviour of a Xanthenol Host Compound: Thermal Stability, Kinetics of Desolvation and Guest Exchange Reactions, 38th South African Chemical Institute Conference (38th SACI), Durban, South Africa, 3-8 December 2006.

ABSTRACT

Title: **Inclusion behaviour of related organic host compounds**

Author: Nobathembu Faleni

Date: August 2007

The inclusion behaviour of the two host compounds, 9-(4-methoxyphenyl)-9H-xanthen-9-ol (**A1**) and 9-(4-methylphenyl)-9H-xanthen-9-ol (**A10**) were investigated. These host compounds are large, bulky, rigid and they contain functionalities that allow them to selectively interact with other molecules, such as the guests in this work. The host molecules form inclusion complexes with small organic guest molecules. The host•••guest interactions are the interesting focus of this study.

The host **A1** included the guests: cyclohexane, 1,4-dioxane and N,N-dimethylformamide. Kinetics of desolvation were studied for the 1,4-dioxane and N,N-dimethylformamide compounds. Guest-exchange reactions were performed. The host **A1** was also used in the separation of 1, 4-dioxane and benzene.

The host **A10** included the guests; benzene, 1,4-dioxane, cyclohexane, cyclohexanone, N,N-dimethylacetamide and N,N-dimethylformamide. Kinetics of desolvation were studied for the benzene and cyclohexane compounds. The host **A10** was used in the separation of the following pairs of guests: benzene and 1,4-dioxane; N,N-dimethylformamide and N,N-dimethylacetamide.

The structures of the compounds were elucidated using single crystal X-ray diffraction. Thermal analysis was performed in order to determine the thermal

stabilities of the complexes, including techniques such as thermogravimetry, differential scanning calorimetry and melting point measurement. The reactions in the guest exchange experiments were monitored using differential scanning calorimetry.

Competition experiments were performed to determine the selectivity of a host for a series of related guests. These experiments were conducted between pairs of guests.

Table of contents

CHAPTER 1 INTRODUCTION

Supramolecular chemistry and inclusion compounds

This type of chemistry is involved in diverse disciplines and fields, having complete control over supramolecules, molecular assemblies and materials [1].

Supramolecular Chemistry is the chemistry of multicomponent molecular assemblies. The component structural units are held together by a variety of weaker (non-covalent) interactions [2].

It is highly interdisciplinary in nature and has applications in related fields of physics and biology where it has been used in a considerable number of systems binding organic components into larger assemblies. This has resulted in a change in focus from single molecules, which are constructed step by step through the formation of direct covalent linkages, towards molecular assemblies, with their usual non-covalent weak intermolecular contacts.

Much of the work has focused on molecular design for achieving complementarity between single molecule hosts and guests.

Inclusion Compounds

Inclusion compounds have been known since the beginning of the second last century [3].

In 1811 Sir Humphrey Davy discovered the chlorine hydrate ($Cl_2 \cdot 6H_2O$) of an inclusion compound [4] and was studied by Michael Faraday [5] in 1823. E.Mittscherlich[6] recognized the idea of a polymorphic compound. In 1828 F. Wöhler first synthesized the compound urea [7].

Coordination chemistry was firstly introduced in 1893 by Alfred Werner, implying that the two compounds could bind to one another if there was some kind of interaction. Emil Fischer expanded the process and in 1894 introduced the 'lock and key' concept [8] giving a more visual understanding of molecular recognition. It was in 1912 that Max von Laue first discovered X-ray diffraction [9] and in 1913 the structure of sodium chloride was determined by Bragg [10]. The term 'hydrogen bond' [11] was first used by L. Pauling in 1935, followed by the first mention of the weak hydrogen bond in 1936 by O. R. Wulf [12]. In 1948 H. Powell proposed structures for the ß—quinol inclusion compounds and introduced the term 'clathrate' [13] to describe the total encapsulation of a guest within a host framework cavity.
In 1952 F. Cramer referred to molecules able to enclose other molecules in their structure without covalent bonding as inclusion compounds [14] and recognized that no functional groups and no chemical reaction was needed.

Inclusion compounds can be classified into two categories. A schematic diagram is shown in Figure 1.1.

(a) Molecular inclusion: is the formation of a molecular complex, where a convex guest fits into the cavity of one host molecule.

(b) Lattice inclusion: is the inclusion of guest molecules into the cavities between different host molecules in the crystal lattice (clathrate formation).

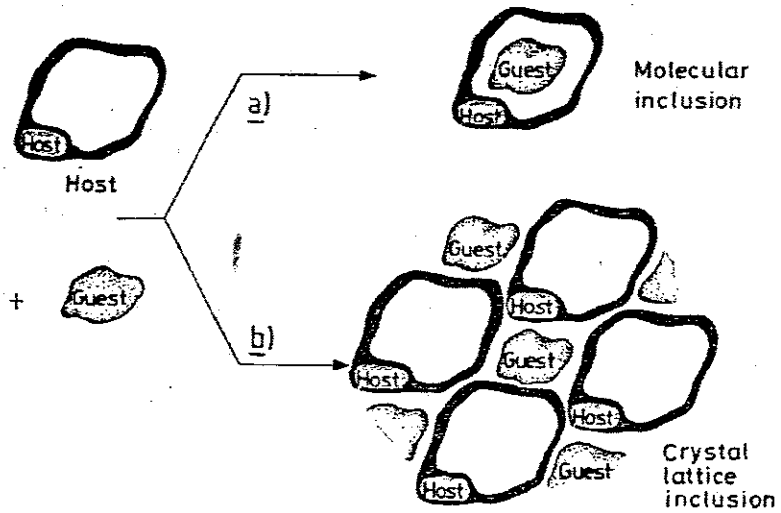

Figure 1.1 Schematic drawing illustrating the two basic types of inclusion [15].

A clathrate is formed when the guest is entirely enclosed by the host framework and is not limited to cage inclusion compounds but can incorporate other shapes as well [16]. Figure 1.2 shows types of voids that are created by the host framework in solid state host-guest compounds [17].

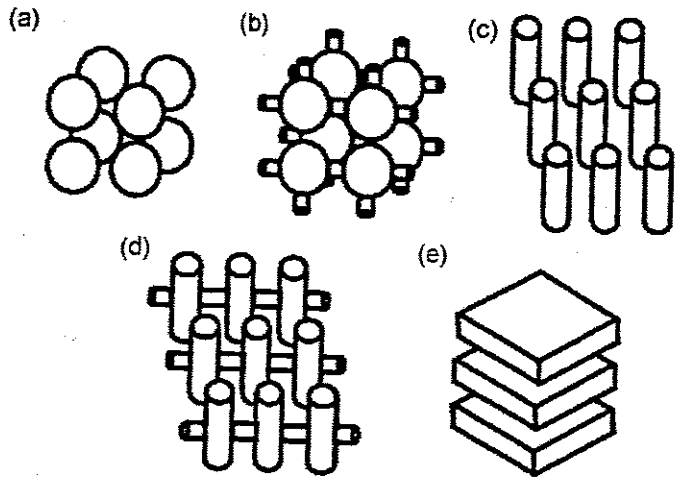

Figure 1.2 Examples of topologies of lattice clathrates; (a) cages or pocket
(b) interconnected cages, (c) channels, (d) intersecting channels
(e) layers

Intermolecular Interactions

The central focus of the field of supramolecular chemistry is the variety of non-covalent interactions such as hydrogen bonding, C—H•••π, π–π stacking, dipole-dipole and van der Waals interactions and hydrophobic binding which are considered to stabilize the various components of a particular complex [18] .

Hydrogen Bonding

The hydrogen bond can be described as D–H•••A, where D is a donor atom, H is a hydrogen and A is an acceptor atom [21-22]. The hydrogen bond plays a major role in the formation of supramolecular systems. Hydrogen bonding occurs most commonly between donor groups (D) such as: C–H, N–H, O–H, F–H, P–H, S–H, Cl–H, Br–H and I–H and acceptor (A) groups such as N, O, P, S, Cl, Br, I, alkenes,alkynes,aromatic π-systems and transition metals [19-20]. Hydrogen bonds are classified as very strong, strong, and weak based on their ability to determine and control supramolecular structure [22]. The hydrogen bond is usually bent, rather than linear as shown in the description above and hydrogen bond parameters are given in Table 1.

Table 1. Typical Parameters of Hydrogen bonds [23].

Hydrogen bond type	Very strong	Strong	Weak
Length H•••A(Å)	1.2 – 1.5	1.5 – 2.2	2.2 – 3.2
< D–H•••A(°)	175 – 180	130 – 180	90 – 150

C–H•••π Interactions

Edge-to-face interactions of aromatic rings fall into this category. In 1998 studies done by Braga [24] on organometallic crystals found average distances from the centroid of the aromatic ring to the oxygen or carbon atom in (C)O–H•••π to be 3.41(3) and 3.69(2) Å respectively. It is understood that this intermolecular interaction stabilizes the crystal structure.

π–π Stacking

This represents the interaction of π clouds of two aromatic rings. This is a directional force as it stabilizes the helical structure of DNA [25], and the packing of the host and guest compounds in crystals. There are two general types of π–π stacking: face- to- face and edge- to- face. In the case of face- to- face interactions the two aromatic rings may not be directly above each other as this is repulsive.

This interaction is attributed to weak electrostatic forces as well as dispersive forces which might be of greater importance [26]. The strength of this interaction varies from 0-50 kJ mol^{-1}.

Van der Waals Interactions

Van der Waals interactions are described as repulsive and dispersive intermolecular forces [23]. The repulsive forces balance the dispersion forces and define molecular shape and conformation. Dispersive forces are attractive in nature and result from the interactions of fluctuating multipoles in adjacent molecules. These forces are non-directional, are less than 5 kJ mol^{-1} in strength and are most important in compounds where small organic guests are included in crystal lattices or molecular cavities.

Host Design

A good host is defined as having the following qualities [26].

- Molecular bulkiness, for a low density packing with the possibility of cavities.
- rigidity, to maintain and sustain cavities
- functional groups, to provide suitable host-guest interactions.

Many organic host compounds have been synthesised based on these principles including those containing hydroxyl functional groups for hydrogen bonding [27-29].

Host molecules can be classified according to their shape and functionality. A few host compounds and their characteristics are given below:

- **Scissor Type Hosts** [30]: These are characterised by the shape of the molecule given in Figure 2. The classic examples of these hosts are:

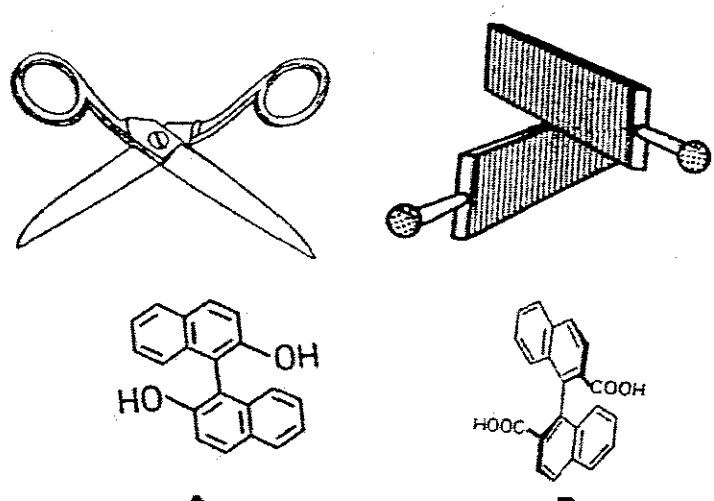

Figure 2. Scissors type hosts [30], **A**: 2,2-dihydroxy-1,1-binaphthyl and **B**: 1,1-binaphthyl-2,2-dicarboxylic acid.

These hosts have been extensively studied, and have been shown to form inclusion compounds with a variety of guests with differing host:guest ratios. Compound **A** enclathrates alcohols, amines, oxides, amides and ketones [31-38]. **B** successfully includes aliphatic alcohols, carboxylic acids and amides [39].

Scissor type host compounds are still extensively studied and a recent paper published by Muraoka *et al.* have described, "reversible operation of chiral molecular scissors by redox and UV light" [40].

- The **Hexa Type Host** [41] is the common feature in the clathrates formed by hydroquinone, phenol and Dianin's compound where the linking of the OH groups of the host molecules forms a hydrogen bonded network such that the oxygen atoms form a hexagonal arrangement. This is illustrated in Figure 3 (a) and compared to (b) hexasubstituted benzene. The hydroxyl group plays a major role in maintaining the 'open' clathrate structure.

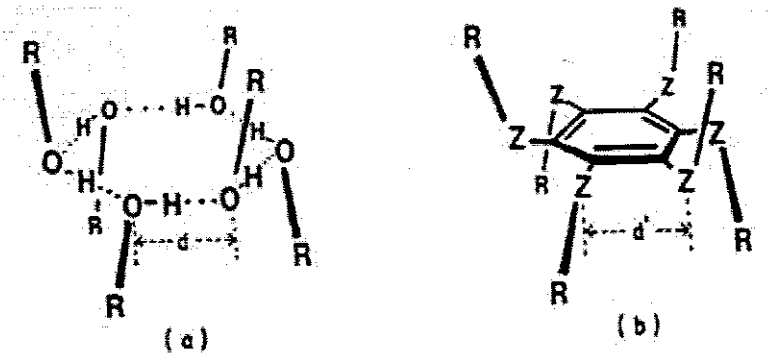

Figure 3. (a) Hexagonal arrangement, (b) hexa substituted benzene

The classic example of the hexa substituted benzene host is hexakis(phenylthio)benzene. This example is shown in Figure 4 and has been found to include a variety of guests with differing host:guest ratios [42]. It has successfully enclathrated carbon tetrachlorides (CCl_4), methyltrichlorides ($CHCl_3$) and bromotrichlorides (CCl_3Br) [43]. Saha *et al.* have discussed an organic hexahost of this type in a paper entitled "Helical water chains in aquapores of organic hexahost: remarkable halogen-substitution effect on the handedness of water helix" [44].

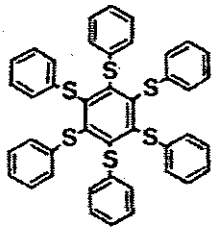

Figure 4. The Hexa Host Type structure, hexakis (phenylthio) benzene.

- A **Cavitand Host** [45] is a single host molecule which possesses an intramolecular cavity and the guest molecule resides completely within the host cavity. An example of a cavitand host is illustrated in Figure 5.

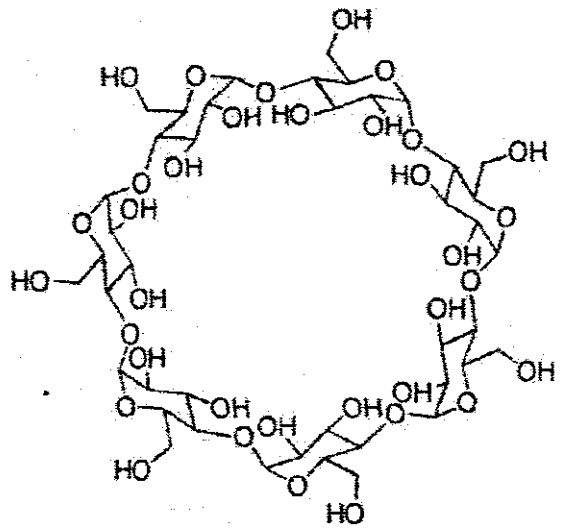

β–cyclodextrin

Figure 5. A typical host for cavitand inclusion formation [45].

Other well studied host molecules of this type include Pederson's crown ethers [46, 47], cyclophanes [48, 49] and calix[n]arenes [50]. Recent work has involved the study of water-soluble cavitands [51] which are desirable because most biological processes occur in water.

Physical Methods of Characterization

Thermal Analysis

Thermal analysis is a very useful tool for the study of inclusion compounds [52-55]. Thermogravimetric analysis (TGA) and differential scanning calorimetry (DSC) are the most common techniques used. A typical TGA experiment measures weight loss as a function of temperature. Each specific weight loss is expressed as a percentage and this allows the calculation of the host to guest ratio. The reproducibility of the weight loss is generally of the order of ± 1%. The onset temperature cannot be determined by TGA because the commencement of weight loss is dependent on particle size and heating rate. TGA is also used extensively in the study of kinetics of desolvation of host-guest compounds. Both isothermal and non-isothermal methods have been employed in this study and are described in Chapter 2.

DSC measures the enthalpy changes of a solid that occur during heating. These enthalpy changes are usually due to guest loss or a phase change. The area under the DSC peak is dependent on the particle size, heating rate, flow rate of the purging gas and the geometry of the calorimeter. The onset temperatures (T_{on}) for a given inclusion compound are dependent on the host-guest interactions and on the inherent physical properties of the guest included.

X-ray diffraction

X-ray diffraction [56] is an essential tool as it allows for the accurate assignment of the positions of the atoms in a crystal structure as well as details about the molecular packing. This technique gives us information about the intermolecular interactions taking place, as an indication of how the structure is stabilized.

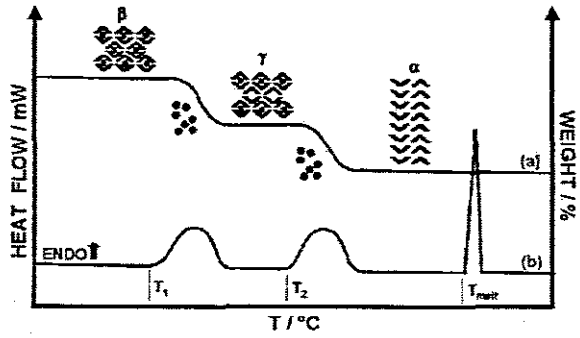

Figure 6. Schematic diagram [57] illustrating (a) TGA and (b) DSC traces.

Guest Exchange Reactions

There are two possible mechanisms for any guest exchange reaction:

(a) $H \bullet nG_{\,I\,(s,\,ß)} + mG_{2\,(\text{liquid or vapour})} \rightarrow H \bullet m\,G_{2(s,\,ß)} + nG_{\,I\,(\text{liquid or vapour})}$

In (a) the host-guest compound retains its structure throughout the exchange reaction. This mechanism is uncommon for organic hosts and the classic example is the host gossypol, which forms a clathrate with dichloromethane as guest, retains its structure on desorption, and absorbs other volatile guests [58].

(b) $H \bullet nG_{\,I\,(s,\,ß)} \rightarrow H_{\,(s,\,\alpha)} + nG_{I\,(\text{liquid or vapour})}$

$H_{(s,\,\alpha)} + mG_2 \rightarrow H \bullet mG_{2(s,\,ß)}$

In (b) the host-guest system desorbs the original guest G_1 to yield the apohost in its α, nonporous phase, which in turn forms a new inclusion compound with the incoming guest G_2. The exchange of *p*-xylene with benzene in the clathrates formed with 9-(3-chlorophenyl)-9H-xanthen-9-ol [59] is an example of this.

Applications of Host-Guest Chemistry

The applications of host-guest chemistry have grown tremendously and have been reported in a set of 10 volumes of 'Comprehensive Supramolecular Chemistry' [60]. Amongst the topics covered are:

- Catalysis, pollution control and storage of reagents.
- Alteration of physical and chemical properties of pharmaceutical drugs by inclusion in cyclodextrins.
- Separation of isomers, chiral resolution, polymerisation and liquid crystals.

Inclusion compounds have found various practical applications [15]:

- In the separation of racemates with the help of urea.
- In pharmacology, for the protection of drugs from oxidation, forms of decomposition and also to effect rapid absorption by the body.
- The fixation of volatile fragrances and drugs.

There is hope that inclusion compounds of pesticides will be safer and easier to handle.

Aspects of this Study

The host 9-(4-methoxyphenyl)-9H-xanthen-9-ol (**A1**) and 9-(4-methylphenyl)-9H-xanthen-9-ol (**A10**), possess similar geometries and a different functionality of methoxy (**A1**) and methyl group (**A10**) in the para-position.
One of the aims of this study was to determine the effect of this on the type of interactions that occur between the host and guest molecules as well as packing arrangements of the crystal structures.

Therefore a wide variety of guests were included according to their size, geometry or acceptor/ donor capabilities. These included aromatic guests like benzene, various six membered aliphatic rings eg. cyclohexane, cyclohexanol and amides eg. N,N-dimethylformamide and N,N-dimethylacetamide. The physical properties of the guests used in this study are listed in Table 2. They are all liquids at room temperature. Separation of certain guests was attempted using the above mentioned hosts in competition experiments between, for example, benzene and 1,4-dioxane.
The thermal stability of the resultant inclusion compounds was investigated and where possible gas chromatography (GC) was used to determine the selectivity of each host for a series of guests. Guest exchange experiments were performed between **A1** inclusion compounds and selected guests.

Physical Properties of Guests Included

The melting points, boiling points and vapour pressures of the guests are given below. The data were obtained from Aldrich Advancing Science [61].

Table 2. Physical Properties of Guests Studied

Guest	Molecular formula	m.p.(°C)	b.p.(°C)	V.p.(mmHg) / temp °C
Benzene	C_6H_6	5.5	80	74.6 / 20
1,4-dioxane	$C_4H_8O_2$	10-12	100-102	27 / 20
N,N-dimethylacetamide	$CH_3CON(CH_3)_2$	-20	165-166	2 / 25
N,N-dimethylformamide	$CHON(CH_3)_2$	-61	153	2.7 /20
Cyclohexane	C_6H_{12}	4-7	80.7	77 / 20
Cyclohexanol	$C_6H_{11}OH$	22	160-161	1 / 20
Cyclohexanone	$C_6H_{10}(=O)$	-47	155	3.4 / 20

References:

1. J.-M. Lehn, *Angew. Chem., Int. Ed.Engl.* (Nobel lecture), 1988, **27**, 89.

2. J. L. Atwood, J. E. D. Davies, D. D. MacNicol and F. Vögtle *Comprehensive Supramolecular Chemistry*, Vol. 1-10, eds., Pergamon, Oxford, 1996.

3. W. Schlenk Jr, Chem.Unserer Zeit, 1969, **3**,120.

4. H. Davy, Philos. *Trans.R.Soc.London.*, 1811, **1**,101.

5. J. W. Steed, J. L. Atwood in *Encyclopedia of Supramolecular Chemistry*, Vol. 2, Marcel Dekker,Inc., New York, **2004**, 1401.

6. E. Mitscherlich, *Abhl. Akad. Berlin*, 1823, **43**.

7. F. Wöhler, *Poggendorfs Ann. Physik*, 1828, **12**, 253.

8. E. Fischer, *Ber. Deutsch. Chem. Ges.*, 1894, **27**, 2985.

9. M. von Laue, *Physics 1901-1921 (Nobel lecture)*, Elsevier Publishing Company, Amsterdam, 1967.

10. L. Bragg, *The development of X-ray Analysis*, Dover: New York, 1975.

11. L. Pauling, *J. Am. Chem. Soc.*, 1935, **57**, 2680.

12. O. R. Wulf, U. Liddel, S. B. Hendricks, *J.Am.Chem.Soc.*, 1936, **58**, 2287.

13. H. J. Powell, *J. Chem. Soc.*1961, **73**, 5691.

14. F. Cramer, *Angew. Chem.* 1952, ***64***, 437.

15. J. L. Atwood, J. E. D. Davies and D. D. MacNicol (Eds), *Inclusion Compounds*, Academic Press, New York,1984.

16. W. Schlenk, Die Harnstoff-Addition der aliphatischen Verbindungen. Ann. Chem., 1949, **565**, 204-240.

17. K. D. M. Harris, Chemistry in Britain, 1993, 132.

18. E. C. Constable and D. Smith, *Chem. Br.*, 1995, 33.

19. G. A. Jeffrey, *An Introduction to Hydrogen Bonding*, Oxford University Press: Oxford 1997.

20. C. B. Aakeröy and K. R. Seddon, *Chem. Soc. Rev.*, 1993, **22,** 397.

21. G. R. Desiraju, T.Steiner, *The Weak Hydrogen Bond in Structural Chemistry and Biology*, Oxford University Press, Oxford, 1999.

22. M. Nishio, M. Hirota, Y. Umezawa. *The CH/π Interaction, Evidence, Nature and Consequences*, Wiley – VCH: New York, 1998.

23. J. W. Steed, J. L. Atwood, *Supramolecular Chemistry*,John Wiley & Sons, Chichester, 2000.

24. D. Braga, F. Grepioni, E. Tedesco, *Organometallics*, 1998, **17**, 2669-2672[136-138,199,271].

25. C. A. Hunter, J. K. M. Sanders, 'The Nature of π– π Interactions', *J. Am. Chem. Soc.* 1990, 112, 5525-5534.

26. E. Weber, *Inclusion Compounds*, Vol.4, Eds J. L. Atwood, J. E. D. Davies and D. D. MacNicol, Oxford University Press, Oxford, 1991,188.

27. F. Toda, K. Tanaka, G. U. Daumas, C. Sanchez, *Chem. Lett.*, 1983, 1521.

28. E. Weber, N. Dörpinghaus, C. Wimmer, Z. Stein, H. Krupitsky, I. Goldberg, *J. Org.Chem.*, 1992, 57, 6825.

29. R. Bishop in Comprehensive Supramolecular Chemistry, Vol.6, eds. D. D. MacNicol, F. Toda, Pergamon, Oxford, 1996, Chapter 6.

30. E. Weber, Inclusion Compounds, Key Host Organic Host Systems. Eds. J. L. Atwood, D. D. MacNicol and J. E. D. Davies, Vol. 4, Chapter 5, Oxford University Press, Oxford, 1991.

31. E. Weber and M. Czugler, Molecular inclusion and molecular recognition, Vol. 149, Chapter2, p.45,Springler-Verlag, Berlin-Heidelberg,1987.

32. F. Toda, Molecular inclusion and molecular recognition, Vol. 140, Chapter3, p.43, Springler-Verlag, Berlin-Heidelberg, 1987.

33. G. H. Lee, Y. Wang, K. Tanaka, M. C. Wong and T. C. Mak, *Chem.Lett.*, 1987, 2069.

34. F. Toda, K. Tanaka and S. Nagamatsu, *Tetrahedron Lett.*, 1987, 2069.

35. F. Toda, K. Tanaka and S. Nagamatsu, *Tetrahedron Lett.*, 1984, **25**, 4929.

36. F. Toda and K. Mori, *J.Chem.Soc.Commun.*, 1986, 1059.

37. K. Mori and F. Toda, *Chem. Lett.*, 1988, 1997.

38. F. Toda and K.Mori, *J. Chem. Soc., Commun.*, 1986, 1357.

39. F. Toda, K. Mori ,Z. Stein and I. Goldberg, *J. Org. Chem.*, 1988, **53**, 308.

40. T .Muraoka, K. Kinbara and T. Aida, *Chem. Commun.*, 2007, **14**, 1441-1443.

41. J. L. Atwood, J. E. D. Davies, D. D. MacNicol, Inclusion Compounds, Structural Aspects of Inclusion Compounds formed by Organic Host Lattices, Vol. 2, Chapter 5, 1984.

42. D. D. MacNicol and D. R. Wilson,*J. Chem. Soc. Commun.*, 1976, 494.

43. F. Vögtle and E. Weber, *Angew. Chem., Int. Ed. Engl.*, 1974, 13, 814.

44. B. K. Saha, A. Nangia, *Chem. Commun.* 2005, 24, 3024-3026.

45. E. Weber and H.-P.Josel, *J.Incl.Phenom.*1983, **1**, 79-85.

46. C. J. Pedersen,*J.Chem.Soc.* , 1967, 89, 2495-2496.

47. C. J. Pedersen, Angew.Chem., Int. Ed. Engl., 1988, 27, 1021-1027.

48. F. Diederich, *Cyclophanes: Monographs in Supramolecular Chemistry*, The Royal Society of Chemistry, Cambridge, UK, 1991.

49. Y. Murakami and O.Hayashida, in Comprehensive Supramolecular Chemistry, ed. F. Vögtle, Pergamon, Oxford, 1996, Vol. 2, 419-438.

50. A. Casnati, D. Sciotto and G. Arena, in *Calixarenes 2001*,ed. Z. Asfari, Kluwer Academic Publishers, The Netherlands, 2001, 440-456.

51. S. M. Biros and J. Rebek, Jr., *Chem. Soc. Rev.*, 2007, 36, 93-104.

52. M. E. Brown, *Introduction to Thermal Analysis*,Chapman & Hall,London,1988.

53. B. Wunderlicht, *Thermal Analysis*, Academic Press, San Diego, 1990.

54. P. J. Haines, Thermal Methods of Analysis. Principles, Application and Problems, Chapman & Hall, London, 1995.

55. H. K. Commenga and M. Eppel, *Angew. Chem. Int. Ed. Engl.*, 1995, 34, 1171.

56. COLLECT, Data Collection Software; Nonius: Delft, The Netherlands, 1998.

57. M. R. Caira, L. R .Nassimbeni, in Comprehensive Supramolecular Chemistry, Vol. 6 Solid-State Supramolecular Chemistry Eds. D. D. MacNicol, F. Toda and R.Bishop, Pergamon, 1996.

58. B. T. Ibragimov, S. A. Talipov, T. F. Aripov, *J. Inclusion Phenom. Mol. Recognit .Chem.* 1994, **17**, 317-2124.

59. G. Ramon, A. W. Coleman, L. R. Nassimbeni, B. Taljaard, *Cryst.Growth Des.* 2005, **5**, 2331-2335.

60. J. L. Atwood, J. E. D. Davies, D. D. MacNicol and F. Vögtle, Comprehensive Supramolecular Chemistry, Vol. 1-10, 1996.

61. Aldrich Advancing Science, Handbook of Fine Chemicals, South Africa, 2007-2008.

CHAPTER 2 EXPERIMENTAL

Host Compounds

The two host compounds, 9-(4-methoxyphenyl)-9H-xanthen-9-ol, **A1** , and 9-(4-methyl-phenyl)-9H-xanthen-9-ol, **A10**, were synthesised by Jana Taljaard of the Nelson Mandela Metropolitan University.

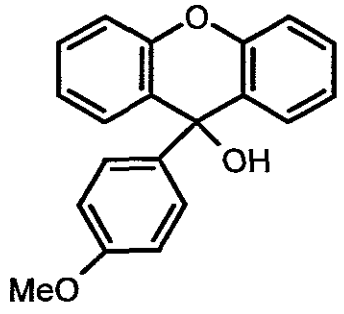

Figure 2.1 Schematic representation of **A1**.

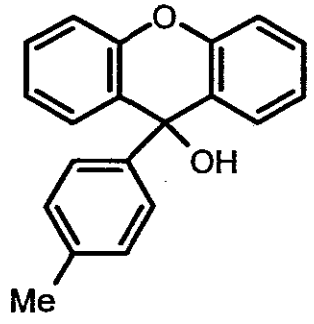

Figure 2.2 Schematic representation of **A10**.

Guest Compounds

Benzene was supplied by BDH Chemicals Ltd England; cyclohexane, cyclohexanone, 1,4-dioxane, N,N-dimethyl acetamide and N,N-dimethyl formamide were supplied by Merck & Co. All solvents were dried using molecular sieves. Benzene and 1,4-dioxane were distilled for the competition experiments.

Crystal Growth

The host compounds were dissolved and heated in the liquid guests to give dilute solutions at 333 K. Both A1 and A10 had low solubility in cyclohexane and a small amount of ethanol was added as a co-solvent. The solutions were left to cool to room temperature resulting in the formation of crystals and after cooling were sealed with parafilm.

Thermal Analysis

Thermogravimetric analysis (TGA) and Differential Scanning Calorimetry (DSC) were performed on a Perkin-Elmer Pyris 6 system. Samples of the crystals taken from the mother liquor were blotted dry with filter paper and crushed before analysis. TGA measures weight loss of the inclusion compounds as a function of time or temperature under controlled conditions. It was also used to study the kinetics of desolvation using both isothermal and non-isothermal methods. DSC measures thermal decomposition, the onset temperatures of the inclusion compounds and the melting point of the host.

The DSC instrument was calibrated using indium (onset temperature, T_{on} = 156.6°C).

TG and DSC experiments were performed at temperatures of 303-573 K at a heating rate of 10 K min^{-1} under flowing dry nitrogen at 20 ml min^{-1}. Sample sizes of 3-5 mg were placed in 50 µl pierced aluminium pans and nitrogen gas was used as the inert atmosphere. The sample size, flow rate and heating rate of the purge gas influence the TGA and DSC results[1].

Kinetics

Isothermal and non-isothermal methods were utilized for determining the kinetics of decomposition of the host-guest compounds studied. These two methods are recognized and have been used comprehensively. The outlines of both methods are given below. For the kinetic studies crystals and powders were used. The powders were formed from stirred solutions of host in the liquid guest and crystals were crushed to limit the outcome of particle size on the results. It is preferred to grow powdered samples since this limits the effect of particle size on the activation energy and results in a more consistent particle

size distribution. From the literature, it can be seen that sample size affects the onset temperature of guest release which would change the kinetics of desolvation[2]. If it is not possible to grow powders then crystals are crushed for analysis.

Isothermal Kinetics

Sequences of TG runs were carried out at selected temperatures. The resultant TG runs were converted into α vs time curves, and fitted to different kinetic models. The α vs time curves can be acceleratory, sigmoidal or deceleratory[2] and can be explained by definite rate expressions.

Table 2.1 lists the kinetic models that have been obtained from Brown[2]. The Arrhenius equation was used to determine the activation energy for the reactions.

Arrhenius equation: $\ln k = -E_a/RT + \ln A$

where k = rate constant,

E_a = activation energy,

A = pre-exponential factor

and T = absolute temperature

Non Isothermal Kinetics

Sequences of ramped TG runs were performed over selected temperature ranges and at different heating rates. Flynn and Wall[3] developed this method for the analysis of the thermogravimetric rate, which is the rate of weight loss against temperature. The thermogravimetric rate is explained by the equation: $dC/dT = (A / \beta) f(C) e^{-E / RT}$, where C = degree of mass loss and β = heating rate.

Then reduced to: $d \log \beta / d\, 1/T \equiv (0.457 / R) E$. An activation energy range can be obtained from plots of $(-\log \beta)$ vs $1/T$.

Table 2.1 Significant rate equations for solid state reactions.

	$f(\alpha) = kt$
1. **Acceleratory**	
P1 power law	$\alpha^{1/n}$
E1 exponential law	$\ln \alpha$
2. **Sigmoidal**	
A2 Avrami-Erofeev	$[-\ln(1-\alpha)]^{1/2}$
A3 Avrami-Erofeev	$[\ln(1-\alpha)]^{1/3}$
A4 Avrami- Erofeev	$[-\ln(1-\alpha)]^{1/4}$
B1 Prout Tompkins	$\ln[\alpha / (1-\alpha)]$
3. **Deceleratory Geometric Models**	
R2 contracting area	$1-(1-\alpha)^{1/2}$
R3 contracting sphere	$1-(1-\alpha)^{1/3}$
Diffusion Models	
D1 one-dimensional	α^2
D2 two-dimensional	$(1-\alpha)\ln(1-\alpha) + \alpha$
D3 three-dimensional	$[1-(1-\alpha)^{1/3}]^2$
D4 Ginstling-Brounshtein	$(1-2\alpha/3) - (1-\alpha)^{2/3}$
Order of reaction models	
F1 first order	$-\ln(1-\alpha)$
F2 second order	$1/(1-\alpha)$
F3 third order	$[1/(1-\alpha)]^2$

α= fraction decomposed

$$\alpha = \left(\frac{m_i - m}{m_i - m_f} \right)$$ and m_i = initial mass

m_f = final mass

Characterisation

Fisher-John Apparatus

Crystals were placed on a Marienfeld 22x22 cm cover glass and covered with a drop of silicone oil.
Upon heating, crystals were monitored to determine decomposition temperatures and observe the changes that occur in the crystal. If, during heating, bubbles were observed this signified that an inclusion compound had been formed.

Competition Experiments

Two component competition experiments classified as competition between two guests were carried out on selected host-guest systems.

In the two component competition, a series of 11 vials were set up containing mixtures of two guests such that the mole fraction of one guest was increased in the range from 0 to 1. The host compound was added and dissolved by heating. The total guest:host ratio was kept at least at 10:1 such that the guest was always in excess. The solutions were allowed to cool to room temperature then closed and sealed with parafilm over a period of a few days. The resultant crystals were dried on filter paper, dissolved in chloroform and placed in vials. The dissolved crystal was absorbed using a 10 µl syringe and 1 µl of the concentration was injected and analysed by gas chromatography. The original mother liquors were also analysed by gas chromatography. Calibration curves were drawn and area concentrations were plotted against mol fraction of 0.1 to 1.

Guest Exchange

Initial compounds H•G1(s) were exposed to vapours of another guest G2 (solvent) in a tight sealed container as shown in the diagram below. DSC was used to monitor the reaction over a time period which varied from a few hours to a few days. All experiments were carried out at room temperature.

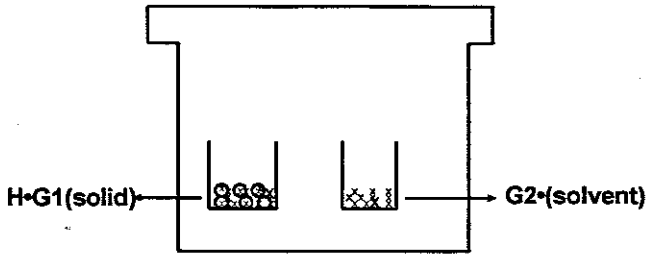

Gas Chromatography

Gas chromatography (GC) was performed on an Agilent 6890N gas chromatograph. Analyses were performed on a polar Carbowax capillary column (30m x 320µm x 0.25µm). The computer package ChemStation[4] was used to monitor and analyse the results. The vials containing mixtures of guests and those containing the original mother liquors were analysed. The gas chromatograph was calibrated using mixtures of known concentrations.

X-ray Powder Diffraction (PXRD)

Powder samples were placed on X-ray insensitive Mylar film. Samples were then mounted on a Huber D-83253 Imaging plate appliance fitted with a Guinier Camera 670, a Huber MC 9300 power supply unit and a Phillips X-ray generator. The generator settings were kept constant at 20 mA and 40 kV while the sample was bombarded with CuKα radiation (λ = 1.54059Å).

We were experiencing technical problems with the PXRD instrument which resulted in a large noise:signal ratio and gave results which looked amorphous. See Figure 3.6 and Figure 3.11.
However the TG trace of the powder matched that of the crystal.

Crystal Structure Analysis

The crystal unit cell parameters and crystal system were determined on a Nonius Kappa CCD diffractometer using 1.2 kW monochromated MoKα radiation (λ = 0.7107 Å) generated by a NONIUS FR590 generator[5] operated at 53 kV and 23 mA. Data collections were done at room temperature, typically at 293-295 K, or at low temperature (113 K).

The space groups were determined by using the collected intensities and pre-determined cell parameters as inputs to the XPREP program[6].
The graphical user interface X-Seed v1.5 was used to run SHELXS-97[7] to solve the crystal structures. Structural models were refined in SHELXL-97[8] and were achieved using full matrix least-squares minimization of the function:

$$\sum W\left(F_0^2 - kF_C^2\right)^2$$

(the weighted sum of the squares of the differences between the observed and the calculated intensities).
The agreement between the observed (F_0^2) and the calculated (F_C^2) structure factors were monitored by assessing the residual index R, defined by R_1 or wR_2.

$$R_1 = \frac{\sum \| F_O | - | F_C \|}{\sum | F_0 |}$$

To give a satisfactory model, both the R_1 and the wR_2 indices should be low when the calculated intensities of the refinement express the agreement against the observed intensities and the measured structure factors are weighted according to their reliability.

$$wR_2 = \left[\frac{\sum w\left(F_0^2 - F_C^2\right)^2}{\sum w\left(F_0^2\right)^2} \right]^{\frac{1}{2}}$$

The weighting scheme w was used to yield a constant distribution in terms of a and b, and further refined in the final cycles of structure refinement.

$$w = \frac{1}{\sigma^2\left(F_0^2\right) + (aP)^2 + bP}$$

and $$P = \frac{\max\left(0, F_o^{\,2}\right) + 2F_c^{\,2}}{3}$$

SHELXL-97[8] refines against F^2, which leads to greater deviations of the Goodness of Fit, S, from unity than the refinement against F.
The Goodness of Fit is expressed as follows:

$$S = \left[\frac{\sum w\left(\left|F_O\right|^2 - \left|F_C\right|^2\right)^2}{\left(N - n_p\right)}\right]^{\frac{1}{2}}$$

where N is the number of reflections and n_p is the total number of parameters refined.

Computational

X-ray powder patterns were calculated using LAZY PULVERIX[9] and compared to experimental powder patterns for characterization. All the crystal packing diagrams were generated with POV-Ray[10]. The program LAYER[11] was utilized to test out systematic absence and space group symmetry. For verification of types of voids occupied by guest molecules, the program SECTION[12] was used to slice through cross sections of the unit cell. In a typical example the host molecules were represented in van der Waals radii with the guest molecules excluded. X-SEED[13] was used as a graphical interface for the programs SHELXS-97, SHELXL-97, LAZY PULVERIX, Pov-Ray, LAYER and SECTION.
The Cambridge Structural Database[14] (CSD) was used to search and analyse published crystal structures.

Table 2.2 Host-guest compounds studied in this thesis.

For Host **A1**

Compound	Guest	H:G ratio
A1·CHEX	cyclohexane	1:½
A1·DIOX	1,4-dioxane	1:½
A1·DMF	N,N -dimethylformamide	1:1

For Host **A10**

Compound	Guest	H:G RATIO
A10·BENZ	benzene	1:½
A10·CHEX	cyclohexane	1:½
A10·CHEXONE	cyclohexanone	1:1
A10·DIOX	1,4-dioxane	1:½
A10·DMA	N,N -dimethylacetamide	1:1
A10·DMF	N,N- dimethylformamide	1:1

References

1. M. R. Caira, and L. R. Nassimbeni, "Phase transformation in inclusion compounds, kinetics and thermodynamics of enclathration" in D.D. MacNicol, F. Toda and R. Bishop(eds.), Comprehensive Supramolecular Chemistry, Vol 6.Solid State Supramolecular Chemistry: Crystal Engineering, Pergamon, Elsevier Science Ltd., Oxford, 1996, 825-850.

2. M. E. Brown, *Introduction to Thermal Analysis,* Chapman & Hall, London, 1988.

3. J. H. Flynn, L. A .Wall, *Polymer Letters,*Vol. 4, 1966, 323-328.
4. ChemStation, Rev., A.10.02 [1757], Copyright©Agilent Technologies 1990-2003.

5. Collect, data collection software, Nonius, 1998.

6. XPREP –Data Preparation and Reciprocal Space Exploration, *Version 5.1/NT*, Bruker Analytical X-ray Systems, 1997.

7. G. M. Sheldrick, SHELX-97, University of Göttingen, 1997.

8. G. M. Sheldrick and T.R. Schneider, *Macromol.Crystallogr.*,1997,B277, 319- 343.

9. K. Yvon, W. Jeitschoko, E. Parthe, *J. Appl. Cryst.*, 1977, 10,73.

10. Pov-Ray for Windows, Version 3.1e.watcom.win32, The persistence of vision development team, ©1991-1999.

11. L. J. Barbour LAYER, A. computer program for the graphic display of intensity data as simulated precession photographs, *J.Appl.Cryst.*, 1999, 32, 351.

12. L. J. Barbour, SECTION, A computer program for the graphic display of cross sections through a unit cell, *J.Appl.Cryst.*, 1999, 32,351.

13. L. J. Barbour, X-Seed, *A graphical interface to SHELX,* University of Missouri, Columbia, USA, 1999.

14. Cambridge Structural Database and Cambridge Structural Database System, Version 5.22 (2001), Cambridge Crystallographic Data Centre, University Chemical Laboratory, Cambridge, England.

CHAPTER 3 A1 AND ITS INCLUSION COMPOUNDS

The inclusion compounds formed between the host, A1, and the guests cyclohexane (CHEX), 1,4-dioxane (DIOX) and N,N-dimethylformamide (DMF) will be discussed.

The crystal structures, thermal stabilities and kinetics of desolvation were studied.

Labelling of the host, **A1**, is given below with the guests included.

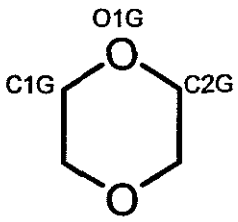

1, 4-dioxane

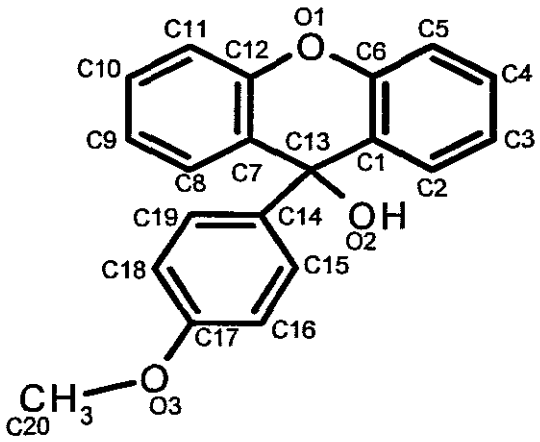

9-(4-methoxyphenyl)-9H-xanthen-9-ol (A1)

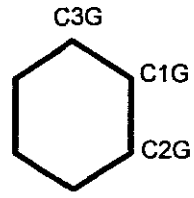

cyclohexane

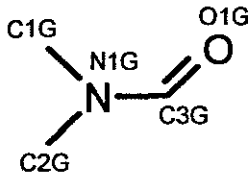

N, N-dimethylformamide

Figure 3.1 A schematic diagram of the host, **A1**, and guests.

The host, **A1**, was dissolved in the liquid guests to give dilute solutions. **A1** is only slightly soluble in cyclohexane and a co-solvent, ethanol, which does not form an inclusion compound with the host, was added until a clear solution was obtained. The solutions were left to evaporate slowly at room temperature until suitable crystals were formed.

Table 3.1 Crystal Data, experimental and refinement parameters.

	A1•CHEX	**A1•DIOX**	**A1•DMF**
Molecular formula	$C_{20}H_{16}O_3 \cdot ½C_6H_{12}$	$C_{20}H_{16}O_3 \cdot ½C_4H_8O_2$	$C_{20}H_{16}O_3 \cdot C_3NOH_7$
Guest	Cyclohexane	dioxane	N,N-dimethylformamide
Host:guest ratio	1:½	1:½	1:1
M_r/g mol^{-1}	346.41	348.38	377.42
Crystal symmetry	Triclinic	Triclinic	Triclinic
Space group	P-1	P-1	P-1
a/Å	8.4834(17)	8.4075(17)	9.0685(18)
b/Å	9.1242(18)	9.0908(18)	9.6815(19)
c/Å	12.712(3)	12.442(3)	12.311(3)
α/°	96.10(3)	97.04(3)	72.36(3)
β/°	104.73(3)	101.33(3)	73.95(3)
γ/°	110.41(3)	111.15(3)	78.05(3)
Z	2	2	2
V/Å^3	871.0(4)	849.9(4)	980.9(4)
μ(Mo-Kα)mm^{-1}	0.086	0.093	0.087
Temperature/K	113(2)	113(2)	113(2)
Range scanned,	2.44-25.64	2.68 – 26.37	3.02- 25.69
Index range	h:-10,9; k:-10,11; l:±15	h:±10; k: ±11; l:±15	h:0,11; k:±11; l:-13,15
No. reflections collected	5676	6199	3695
No. unique reflections	3263	3422	3695
No. reflections with I>2σ(I)	2572	2419	2813
Data/restraints/ parameters	3263 / 2 / 240	3422 / 2 / 240	3695/ 2/ 260
Goodness of fit, S	1.044	1.030	1.033
Final R indices (I>2σ(I))	R_1 = 0.0383, wR_2=0.0955	R_1 = 0.0396, wR_2 = 0.0854	R_1 = 0.0416, wR_2 = 0.1010
R indices (all data)	R_1 = 0.0523, wR_2=0.1026	R_1 = 0.0682, wR_2 = 0.0943	R_1 =0.0607, wR_2 = 0.1096
Largest diff peak and hole (e.Å^{-3})	0.165 and -0.235	0.223 and 0.220	0.177 and 0.247

A1•CHEX

$C_{20}H_{16}O_3$•½C_6H_{12}
Guest: cyclohexane
Space Group: P -1
a=8.483(17) Å α= 96.10(3) °
b=9.124(18) Å β= 104.73(3) °
c=12.71(3) Å γ=110.41(3) °
Volume= 871.0(4) $Å^3$
Z=2

Crystal Structure and Refinement

The crystal unit cell parameters of **A1•CHEX** were obtained from a Nonius Kappa CCD diffractometer. The crystal structure showed that it belongs to a triclinic system with space group P -1. The TG curve confirmed that the inclusion compound has a 1:½ host guest ratio.

The crystal structure was solved by direct methods. The non-hydrogen atoms were found in the difference map. All non-hydrogen atoms of the host and guest were refined anisotropically.
The unit cell contains of two host molecules and one guest molecule (Z=2). The host atoms were found in general positions and the guest was found on a centre of inversion. All hydrogen atoms were found in the electron density maps including the hydroxyl hydrogen of the host. Aromatic hydrogens were fixed at distances of C–H= 0.95 Å. The guest CH_2– hydrogens were fixed with C–H distances of 0.99 Å. The hydroxyl hydrogens were refined isotropically and were placed in calculated positions using the correlation between O–H distances and O•••O distances[1]. The bond angles and bond lengths are all in accepted ranges[2].

Table 3.2 Hydrogen bonding details of **A1•CHEX**.

Donor (D)	Acceptor (A)	D•••A/Å	D-H/Å	H•••A/Å	D-H•••A/
O2	O1[a]	2.865(2)	0.961(1)	1.904(1)	178(2)

[a]: -x,-y+1,-z+2

Crystal Packing

The host molecules form dimers of the form (Host)—OH•••O—(Host). Thus, hydrogen bonding was observed between the hydroxyl oxygen of one host and the ether oxygen of a neighbouring host. These host dimers are located in columns along the [011] direction. The guest molecules lie in constricted channels formed by the packing of the *p*-methoxy phenyl moieties of the host which are effectively cavities. The cavities were mapped using the program SECTION[3] and the dimensions of each cavity were approximately 5.09 Å x 6.76 Å x 6.36 Å.

The cyclohexane molecule lies on a centre of symmetry at Wyckoff position *a* and exhibits the expected chair conformation. No significant contacts between guest and host molecules were detected, thus this is a true clathrate structure. The closest C-H•••π contact between the host and the guest is 3.689 Å. This is the distance from C1G to the centroid of one of the aromatic rings of the host molecule defined by (C7, C8, C9, C10, C11, and C12). The angle C1G—H1G•••centroid is 138.21°. This compares favourably with the average value of 3.69(2) Å given by Braga[4] for a C—H•••π distance with the average angle given as 142(2) °.

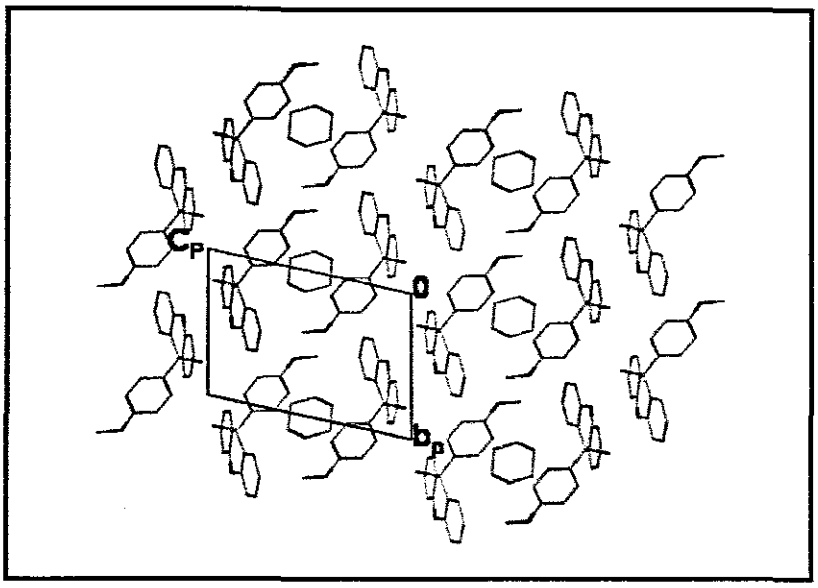

Figure 3.2 Packing diagram of **A1•CHEX** down [100].

Thermal Analysis

The DSC curve gave two endotherms of which the first (T_{on}=380.2K) corresponds to the loss of guest and the second (T_{on}=390.4K) is due to the host melt.

The TG curve showed two steps which individually do not correspond to a stoichiometric loss of guest. The first step is consistent with the loss of 0.35 of the total guest and the second step corresponds to the loss of 0.64 of the total guest. The total experimental guest loss was 13.7% (calculated guest loss= 12.1%).

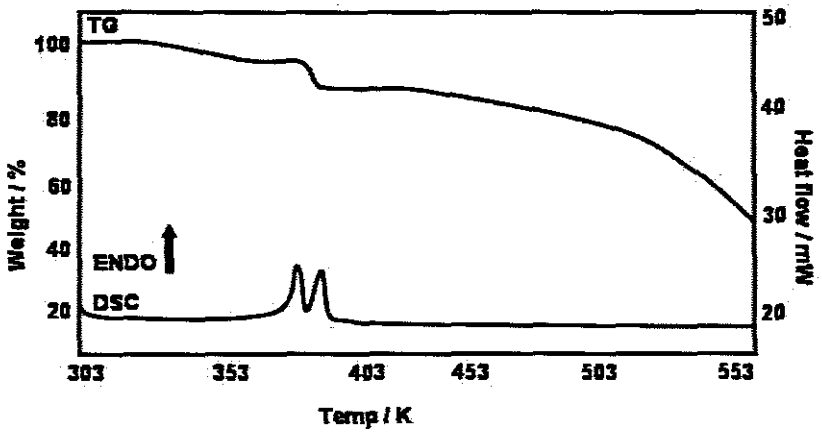

Figure 3.3 TG and DSC curves for **A1•CHEX**.

A1•DIOX

$C_{20}H_{16}O_3$•½$C_4H_8O_2$
Guest : 1, 4-dioxane
Space Group: P -1
a=8.4075(17)Å α= 97.04(3) °
b=9.0908(18) Å β= 101.33(3) °
c=12.442(3) Å γ=111.15(3) °
Volume= 849.9(4) $Å^3$
Z=2

Crystal Structure and Refinement

The TG analysis verified a host:guest ratio of 1:½. The reflection conditions were the same as those found for **A1•CHEX**. The space group P -1 was assigned.

Again the non-hydrogen atoms of the host and the guest were found in the electron density maps with the host atoms situated in general positions and the guests on centres of inversion. All the hydrogens were treated in exactly the same way as was observed for the **A1•CHEX** structure.

Table 3.3 Hydrogen bonding details of **A1•DIOX**.

Donor (D)	Acceptor (A)	D•••A/Å	D-H/Å	H•••A/Å	D-H•••A/°
O2	O1[b]	2.868(2)	0.970(1)	1.900(1)	176(2)

[b]:-x, -y+1, -z+1

Crystal Packing

A1•CHEX and **A1•DIOX** are isostructural with respect to the host. Again the host molecules form hydrogen bonded dimers with the guest molecules situated in constricted channels. The size of the vacancy occupied by the dioxane guests was determined as 5.25 Å x 6.73 Å x 6.38 Å which compares favourably with the size of the cavities in the cyclohexane compound.

The shortest C–H•••π contacts between the host and the guest are:

- 3.779Å for the distance between C1G and the centroid of one of the aromatic rings of the host molecule defined by (C1, C2, C3, C4, C5, C6), the corresponding angle C1G–H1G2•••centroid is 154.34°.
- 3.792 Å for the distance between C2G and the centroid of the aromatic ring defined by (C14, C15, C16, C17, C18, C19), the angle C2G–H2G1•••centroid is 152.88°.

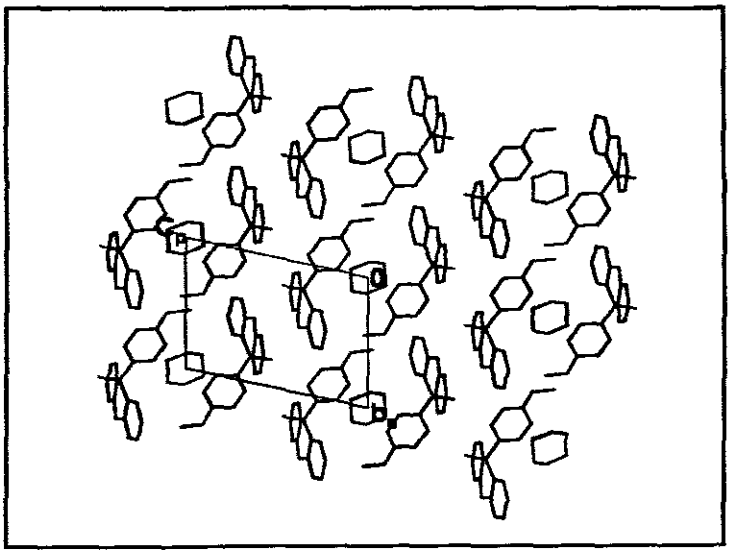

Figure 3.4 Packing diagram of **A1•DIOX** down [100].

Thermal Analysis

A single mass loss step was observed in the TG experiment (Figure 3.5). There is a good correlation between the experimental mass loss which is 12.1% and the calculated mass loss which is 12.6%.
A single endotherm was observed in the DSC due to the host dissolution in the 1,4-dioxane.

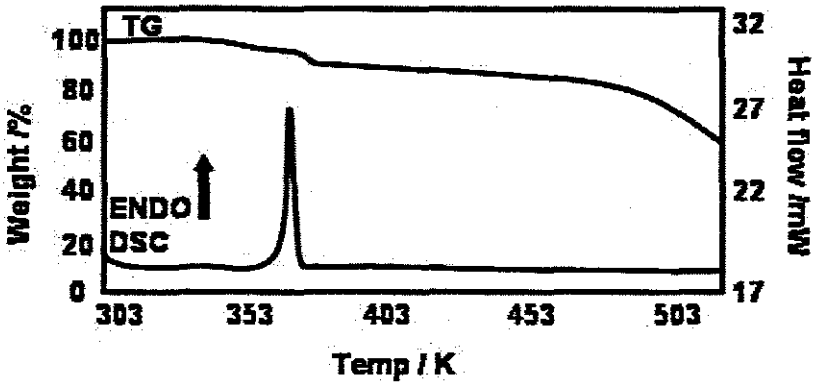

Figure 3.5 TG and DSC curve for **A1•DIOX**.

Kinetics of decomposition

Non-isothermal methods were used to determine the kinetics of desolvation.

Non-isothermal Kinetics

A powder form of **A1•DIOX** was grown at 298 K and the structure was verified using powder x-ray diffraction. There was generally good agreement between the experimentally obtained powder pattern and the calculated one generated from the program LAZY PULVERIX[5]. These are shown in Figure 3.6. TG experiments were performed over a temperature range of 303-473 K at heating rates 1, 2, 5 and 10 K min^{-1}. The TG curves were analysed at percentage mass losses of 2 % to10 % using the Flynn and Wall method[6] and converted into plots of -log β vs 1/T. The activation energy was calculated in the range 133-162 $kJmol^{-1}$.

The host decomposes soon after the guest is released and this results in the decomposition curves of **A1•DIOX** giving inconsistent mass loss values at different temperatures. Thus isothermal kinetics could not be performed.

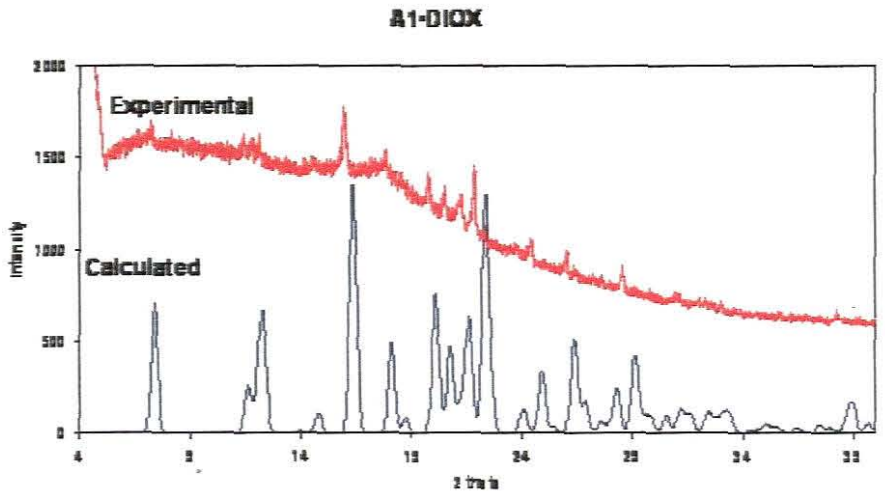

Figure 3.6 Experimental and calculated powder patterns of **A1•DIOX**.

The experimental pattern was obtained at room temperature and calculated one was derived from a structure at low temperatures.

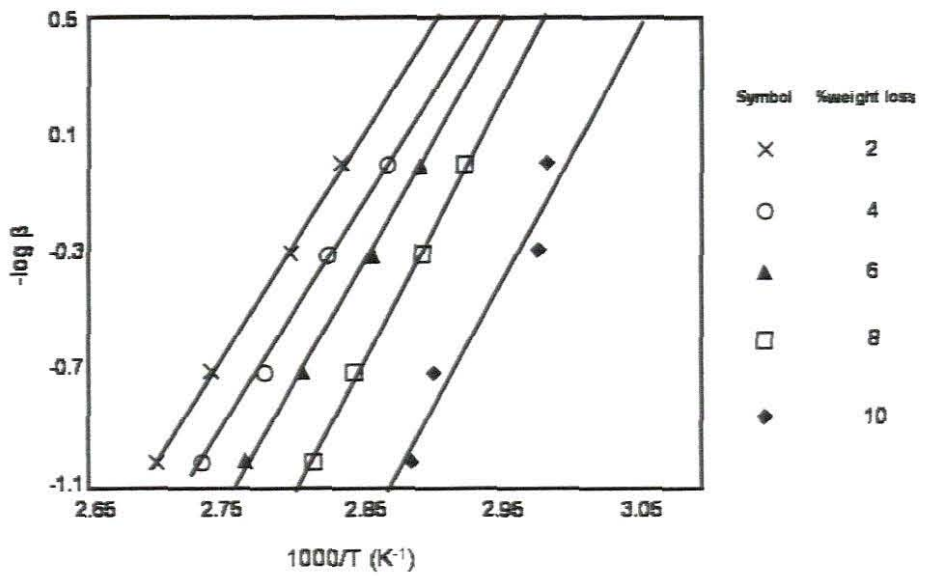

Figure 3.7 Plot of –log β vs. 1/T for **A1•DIOX**.

A1•DMF

$C_{20}H_{16}O_3 \cdot C_3H_7NO$
Guest: N,N -dimethylformamide
Space Group: P -1
a=9.069(17) Å α= 72.36(3) °
b=9.682(19) Å β= 73.95(3) °
c=12.31(25) Å γ=78.05(3) °
Volume= 980.9(4) $Å^3$
Z=2

Crystal Structure and Refinement

TG analysis demonstrated a host:guest ratio of 1:1. The structure was successfully solved in the space group P -1.

All the non-hydrogen atoms of the host and guest were found and refined by direct methods. Both the host and guest molecules were found in general positions. The non-hydrogen atoms of the host were refined anisotropically. The asymmetric unit consists of one host and one guest molecule. The hydroxyl hydrogens were fixed in calculated positions based on the relationship between O•••O distances[1] and O–H distances.

Table 3.4 Hydrogen bonding details of **A1•DMF**.

Donor (D)	Acceptor (A)	D•••A/Å	D-H/Å	H•••A/Å	D-H•••A/°
O2	O1G[c]	2.763(2)	0.960(1)	1.820(1)	167(1)

[c]: -x+2, -y,-z

The hydroxyl hydrogen of the host forms a hydrogen bond with the oxygen of the guest. Two rows of host molecules form a bilayer along [010]. The packing of the host framework provides narrow channels along [100] and [010] which are occupied by the DMF guests.

The dimension of the channels down [100] vary from 6.545 Å x 4.788 Å to 7.745 Å x 8.549Å. The channel down [010] ranges in size from 8.656 Å x 2.736 Å to 8.224 Å x 4.100 Å.

In addition to the hydrogen bonding observed between the host and guest molecules the structure is also stabilised by C—H•••π contacts. In particular we have noted distances which range from 3.435 Å from C3G to the centroid of the aromatic ring of the host defined by C7, C8, C9, C10, C11 and C12, to 3.731Å for the distance between C1G and the C1, C2, C3, C4, C5, C6 aromatic ring of the host. The corresponding C3G—H3G1•••π centroid angle was measured as 152.56° and the C1G—H1G2•••π centroid is 120.91°.

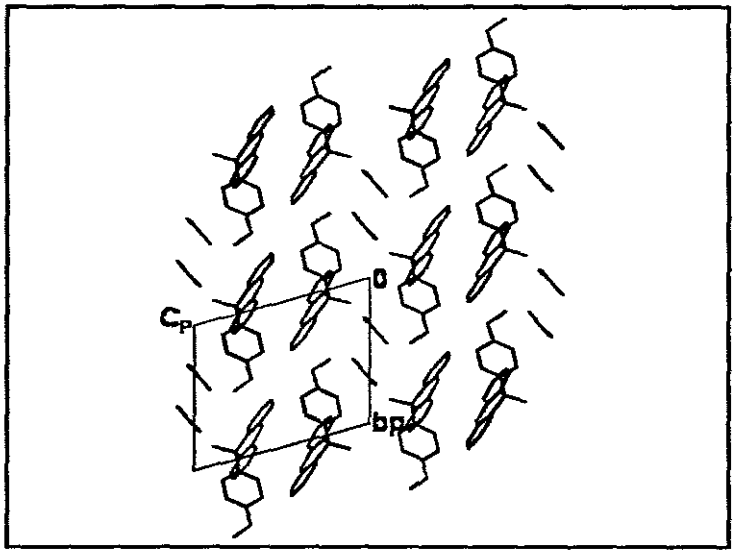

Figure 3.8 Packing diagram of **A1•DMF** along [100]

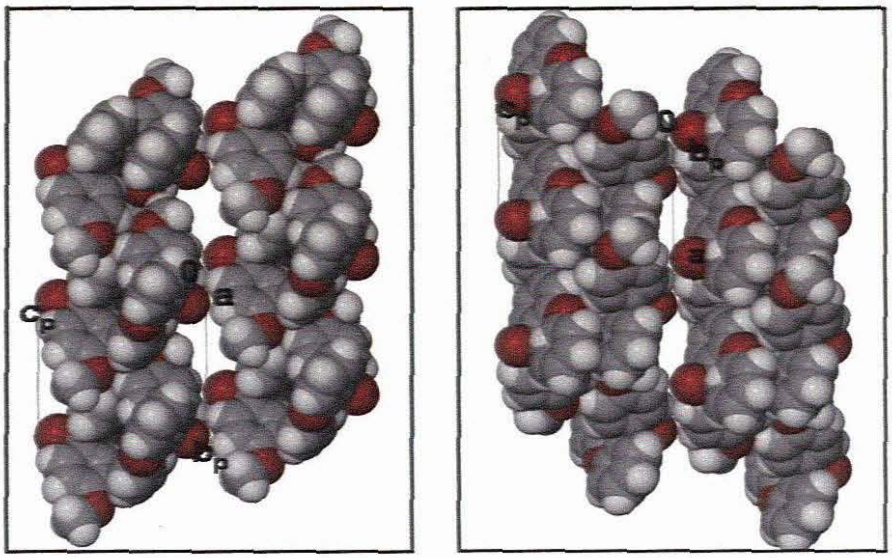

Figure 3.9 Channels of **A1•DMF** showing voids down [100] and [010].

Thermal Analysis

The DSC curve shows one endotherm corresponding to desolvation accompanied by dissolution of the host in the liquid guest.

TG analysis indicated a single mass loss step. The experimental mass loss is 19.7% (*calculated*=19.4%).

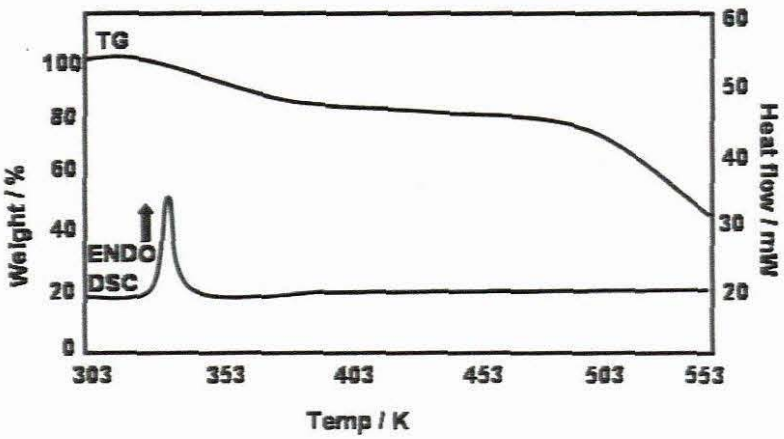

Figure 3.10 TG and DSC curve for **A1•DMF**.

Kinetics of decomposition

Isothermal methods were used to determine the kinetics of desolvation.

Isothermal Thermogravimetry

A series of isothermal experiments were carried out on a powder of **A1•DMF** which was grown at 298 K. There was generally good agreement between the experimentally obtained powder patterns and the calculated ones generated from the program LAZYPULVERIX[5]. These are shown in Figure 3.11. The experiments were conducted at selected temperatures ranging from 323 K to 338 K. The mass loss curves were converted into extent of reaction, α, versus time curves. The α-time curves displayed a fast decomposition step at lower temperatures followed by a slow second step. At higher temperatures the first step controlled the entire reaction and analysis of the first step showed that it followed the deceleratory contracting volume model,

$$R3:\ 1-(1-\alpha)^{1/3} = kt.^{7}$$

The resultant Arrhenius plot is shown in Figure 3.12. An activation energy of 143(15) kJ mol^{-1} was obtained.

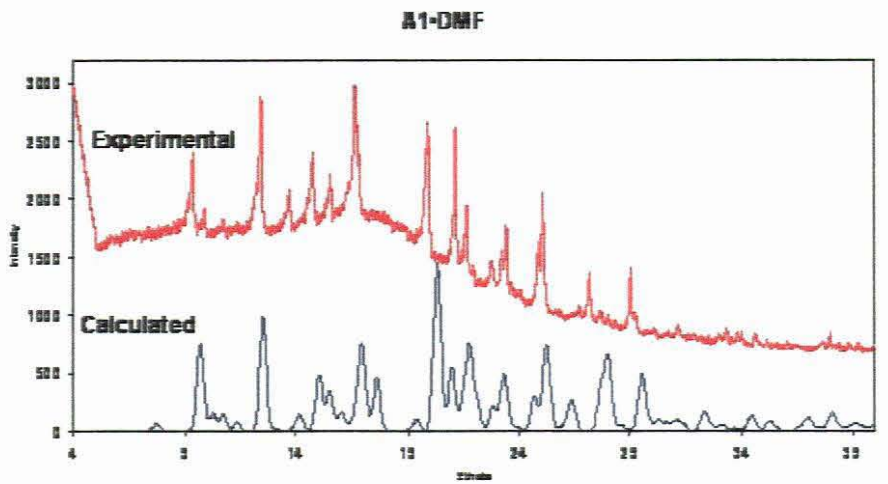

Figure 3.11 Experimental and calculated powder pattern of **A1•DMF**.

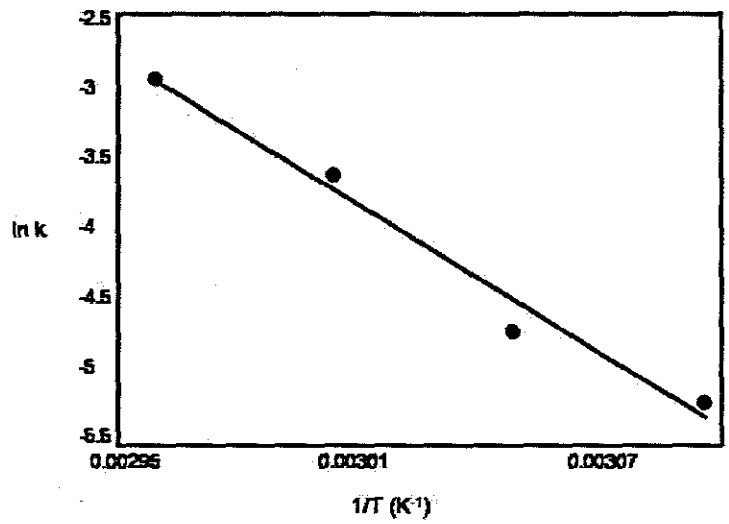

Figure 3.12 Plot of ln k versus 1/T for **A1•DMF**.

Guest Exchange Reactions

Exchange reactions were performed by exposing crushed crystals of each of the inclusion compounds to the vapours of a different guest as described in Chapter 2. In a typical experiment A1•DIOX was exposed to vapours of dimethylformamide in a sealed container at 298 K and the reaction monitored using DSC. Similar experiments were set up between A1•DIOX and cyclohexane, A1•DMF and dioxane, A1•DMF and cyclohexane, A1•CHEX and dioxane and finally A1•CHEX and dimethylformamide.

The overall exchange reaction can be described by the following equation:

$$A1{\bullet}G1_{(S)} + G2\ (vapour) \rightarrow A1{\bullet}G2 + G1\ (vapour)$$

The DSC traces for the complexes are different and thus the reaction was monitored by DSC over a period of 100 min to 2 weeks. The results can be seen in Figures 3.13 to 3.17. The rate of any exchange reaction is generally dependent on particle size and vapour pressure of the incoming guest. The vapour pressures (in mbars)[8] of dimethylformamide, dioxane and cyclohexane at 298 K were 4.39, 49.5, and 130 respectively.

For all of the guest exchange experiments an endotherm due to the host melt was observed at T_{on} = 392 K. This suggests that the reaction proceeded via a

mechanism which involved loss of the guest to yield desorbed host followed by the uptake of the incoming guest. This can be represented by:

$$A1{\bullet}G1_{(S)} \rightarrow A1_{(S)} + G1_{(vapour)}$$

$$A1_{(S)} + G2_{(vapour)} \rightarrow A1{\bullet}G2\ (s)$$

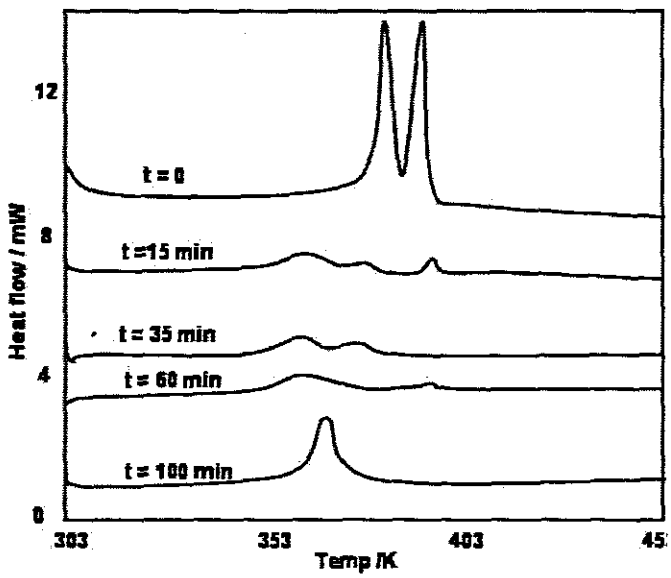

Figure 3.13 DSC results of the exchange reaction represented by:

A1•CHEX(s) + DIOX (g) → **A1•DIOX**(s) + CHEX↑

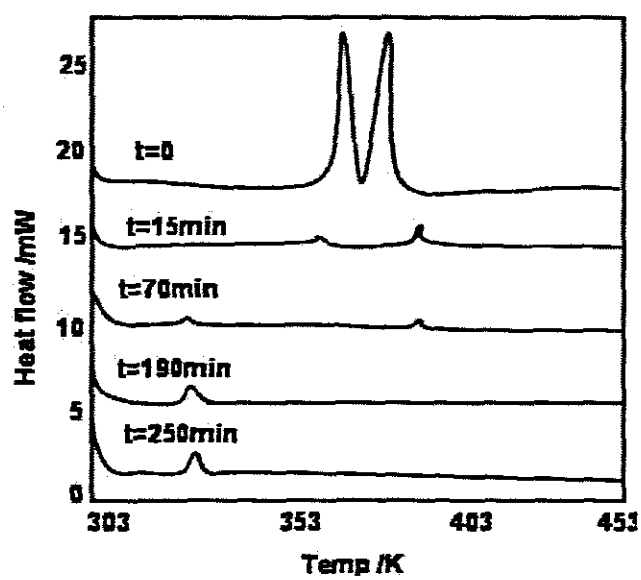

Figure 3.14 DSC result of the exchange reaction:

A1•CHEX(s) + DMF (g) →**A1•DMF**(s) + CHEX↑

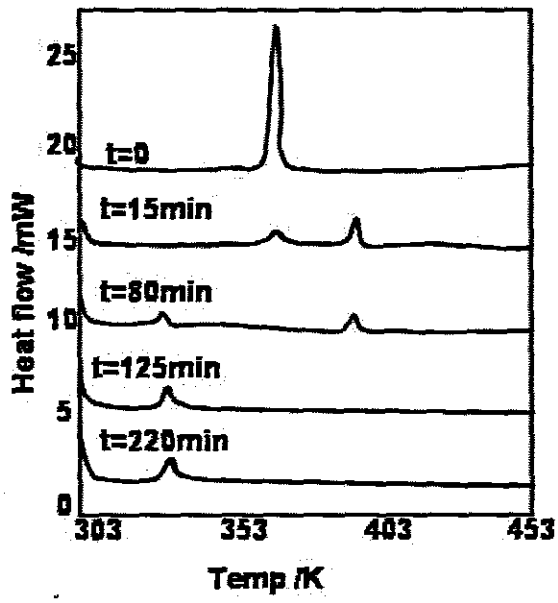

Figure 3.15 DSC results of the exchange reaction represented by:

A1•DIOX(s) + DMF (g) → **A1•DMF**(s) + DIOX↑

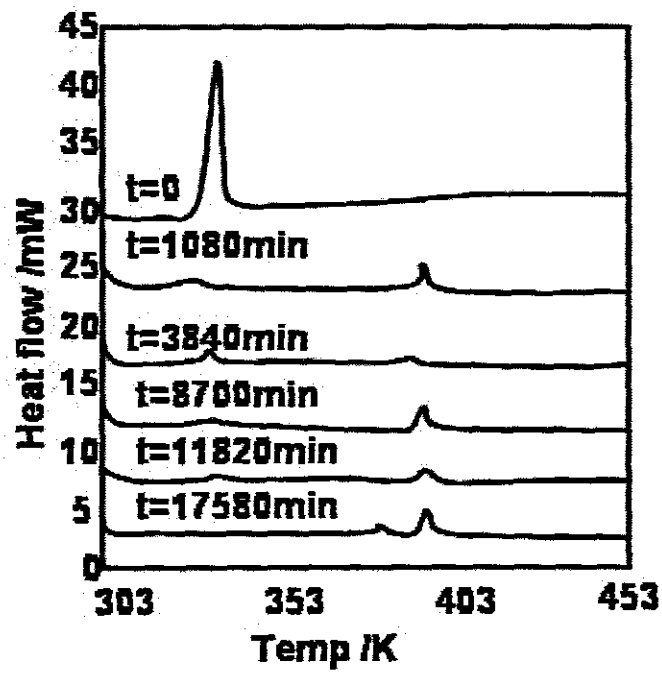

Figure 3.16 DSC results of the exchange reaction represented by:

A1•DMF(s) + CHEX (g) → **A1•CHEX**(s) + DMF↑

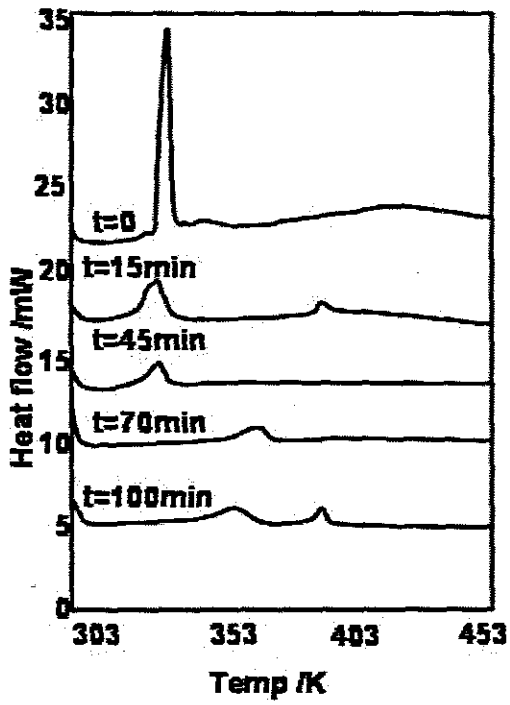

Figure 3.17 DSC results of the exchange reaction represented by:

A1•DMF(s) + DIOX (g) → **A1•DIOX**(s) + DMF↑

Competition Experiments

Two component competition experiments were carried out between benzene and 1,4-dioxane guests. A series of 11 vials were made up with mixtures of guests in a host:guest ratio of 1:10, such that the mole fraction of one guest varied from 0 to 1. The mole fraction of a given guest included by the host versus the mole fraction of the guest in the original mother liquor was plotted. The resultant plot is shown in Figure 3.18. The results show that there is a slight preference of A1 for 1, 4-dioxane. The selectivity is not significant and is within experimental error.

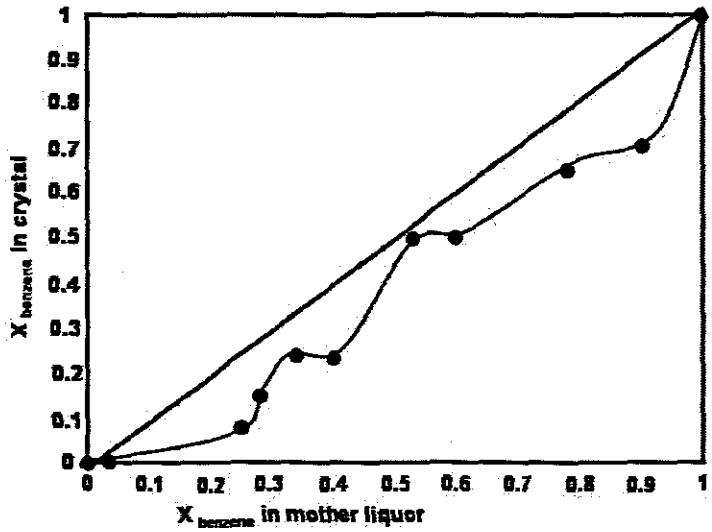

Figure 3.18 Results of competition experiments between A1 and guests, benzene and 1, 4- dioxane.

Discussion

The structures **A1•CHEX** and **A1•DIOX** are isostructural with respect to the host. The host displays the expected packing motif which was previously reported on for inclusion compounds between A1 and benzene, toluene, the xylene isomers[9] and aniline[10]. The host atoms occupy general positions with the guest molecules located on centres of inversion at Wyckoff position *a*. Two host molecules form a centrosymmetric dimer at Wyckoff position *a* (Figure 3.2). The host:guest ratios are typically 1:½ with both the cyclohexane and dioxane guests located in cavities. Stabilisation of the host network occurs via (Host)—OH•••O—(Host) hydrogen bonding.

For the **A1•DMF** structure both the host and the guest atoms were found in general positions with a host: guest ratio of 1:1. This structure displays hydrogen bonding between the host and guest molecules of the form (Host)—OH•••O—(Guest) which is a first for this host. This is illustrated in Figure 3.8. The dimethylformamide molecules are located in interconnected narrow channels running parallel to [100] and [010], Figure 3.9. Both channels exhibit a zigzag arrangement.

Kinetics of desolvation experiments yielded an activation energy range of 133-162 kJmol^{-1} for **A1•DIOX** and 143(15) kJmol^{-1} for **A1•DMF**. These values are in the expected ranges for organic inclusion compounds.

The C—H•••π distances of **A1•CHEX**, **A1•DIOX** and **A1•DMF** are in expected average ranges as mentioned by Braga et al[4].

d = 2.79(2) Å

D = 3.69(2) Å

Angle C—H•••M = 142(2) °

where M is the centroid.

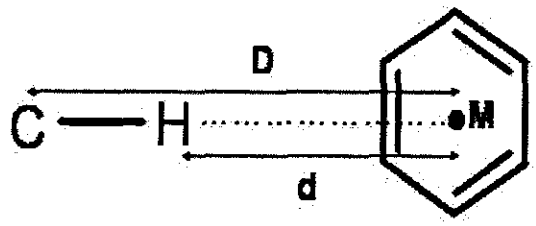

Table 3.5 Summary of thermal analysis data for the structures of **A1** studied.

Inclusion Compound	**A1•CHEX**	**A1•DIOX**	**A1•DMF**
H:G ratio	1: ½	1:½	1:1
TG (calc% mass loss) (exp% mass loss)	 12.1 13.7	 12.6 12.1	 19.4 19.7
DSC T_{on}/**K** Endotherm1 Endotherm 2	 380.2 390.4	 366.2	 331.1
T_b(**K**)	354.2	375.2	426.2
T_{on}/ T_b	1.073	0.976	0.777

DSC results for both **A1•DIOX** and **A1•DMF** show a single endotherm corresponding to dissolution of the host upon release of the guest. The cyclohexane compound, **A1•CHEX**, gave two endotherms, the first due to the guest loss and the second due to host melt. This difference is reflected in the TG results which show single steps for the dioxane and dimethylformamide compounds compared to the two steps of the cyclohexane compound.

These results suggest that **A1•CHEX** undergoes a different, more complex mechanism for thermal decomposition than the other two structures. The ratio of the onset of desolvation (T_{on}) and the normal boiling point (T_b) was used as a measure of thermal stability.

The T_{on}/T_b values as listed in Table 3.5 indicate similar thermal stabilities for **A1•CHEX** and **A1•DIOX** which is expected due to their identical packing arrangements and is comparable to that of **A1•BENZ** clathrate[7] (T_{on}/ T_b =1.039). **A1•DMF** yields a value of T_{on}/ T_b = 0.777, indicating a less stable structure.

There is no significant selectivity of **A1** for either benzene or 1,4-dioxane.

References

1. I. Olovsson, P. Jönsson, *The Hydrogen Bond – Structure and Spectroscopy*, Schuster, G. Zundel; C. Sardify, Eds., North-Holland Publishing Company, USA, 1975.

2. International Tables for Crystallography, Vol.C, Ed., A.J.C. Wilson, Kluwer Academic Publishers, Dordrecht, 1992, pp.691.

3. L. J. Barbour, *SECTION,* a computer program for the graphical display of cross sections through a unit cell, *J.Appl.Cryst.* 1999, **32**, 353.

4. D. Braga, F. Grepioni, E. Tedesco, *Organometallics*, 1998, **17**, 2669-2672[136-137,138,199,271]

5. K. Yvon, W. Jeitschko, E. Parthe, *J.Appl. Cryst.* 1977, **10**, 73.

6. J. H Flynn, L.A Wall, *J.Polym. Sci, Part B: Polym. Lett.*, 1966, **4**,323.

7. M. E Brown, *Introduction to Thermal Analysis*, Chapman and Hall, New York, ch.13.

8. CRC Handbook of Chemistry and Physics, **87**th ed., CRC Press, Taylor and Francis, 2006, Boca Raton,FL, USA.

9. A. Jacobs, L. R Nassimbeni, H. Su; B.Taljaard,. *Org.Biomol.Chem.* 2005, 3, 1319-1322

10. A. Jacobs, L. R. Nassimbeni, J. H. Taljaard, *CrystEngComm*,2006, **7**, 731 734.

CHAPTER 4 A10 AND ITS INCLUSION COMPOUNDS

The host A10 formed inclusion compounds with guests benzene, cyclohexane, cyclohexanone, N,N-dimethylformamide, N,N-dimethylacetamide and 1,4-dioxane. The crystal structures obtained and thermal stability of the inclusion compounds formed will be discussed.

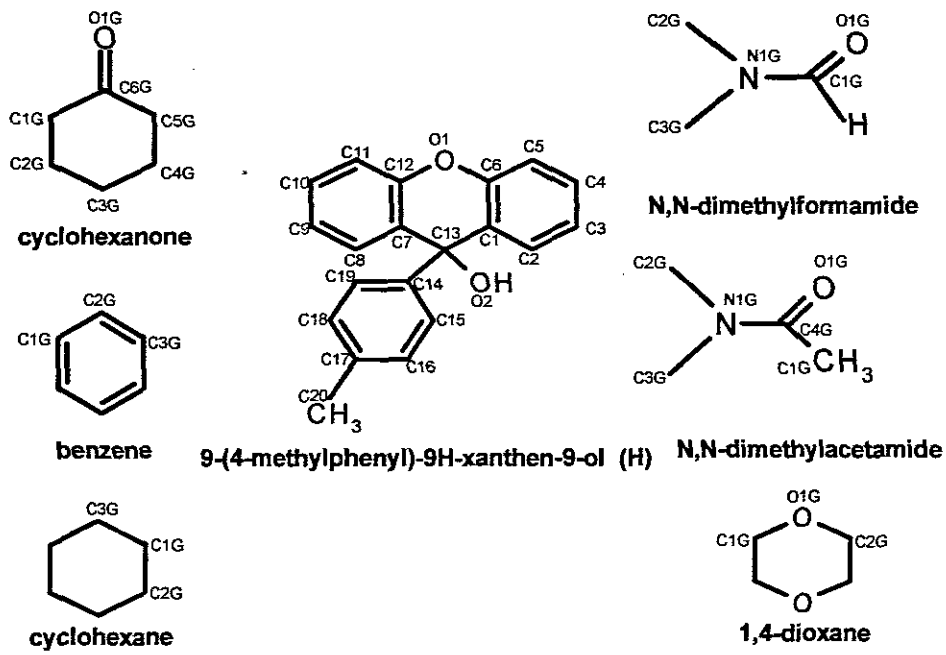

Figure 4.1 A schematic diagram of the host and guests.

The host, **A10,** was dissolved in the liquid guests to give dilute solutions. A10 is only slightly soluble in cyclohexane and a co-solvent, ethanol, which does not form an inclusion compound with the host, was added until a clear solution was obtained. The solutions were left to evaporate slowly at room temperature until suitable crystals were formed.

A10•BENZ

$C_{20}H_{16}O_2$•½C_6H_6
Guest: benzene
Space Group: P -1
a =8.4271(17) Å α =99.86(3) °
b =9.0895(18) Å β =97.55(3) °
c= 11.870(2) Å γ =110, 19(3) °
Volume = 822.7(3) $Å^3$
Z= 2

Crystal Structure and refinement

The crystal unit cell dimensions were established from the intensity data measured on a Nonius Kappa CCD diffractometer using graphite-monochromated Mo-Kα radiation. The **A10•BENZ** structure was solved successfully in the space group P -1. A host:guest ratio of 1:½ was established by TG and this was confirmed by the crystal structure.

All the non-hydrogen atoms of the host and guest were found in the electron density maps and refined anisotropically. The unit cell contains of two host molecules and one guest molecule (Z=2). The hydroxyl hydrogens were located in the difference electron density maps, and were refined isotropically. The hydroxyl hydrogens were placed in calculated positions based on the relationship between O—H and O•••O distances [1]. The remaining hydrogen atoms were geometrically constrained as was described in Chapter 3. The bond lengths and angles of the host molecule are all within accepted ranges [2].

Table 4.1 Hydrogen bonding details of **A10•BENZ.**

Donor (D)	Acceptor (A)	D•••A/Å	D-H/ Å	H•••A/ Å	D-H••• A/°
O2	O1[a]	2.864(2)	0.960(1)	1.907(1)	174(2)

[a]: -x, -y-1, -z-1

Crystal Packing

The crystal packing of **A10•BENZ** is illustrated in Figure 4.2 and is very similar to that observed for **A1•CHEX** and **A1•DIOX**. Hydrogen bonding was observed between the hydroxyl oxygen of one host and the ether oxygen of a neighbouring host. The host forms dimers of the form (Host) — OH•••O (Host). The host dimers form layers parallel to the [011] direction. The guest molecules lie in cavities formed by the packing of *p*-methyl phenyl moieties of the host. The cavity were mapped using the program SECTION [3] and size was found to be 5.27 Å x 5.72 Å x 6.78 Å.

The benzene molecule lies on a centre of symmetry at Wyckoff position *a*. No significant contacts between guest and host molecules were detected, thus this is a true clathrate structure. The closest C-H•••π contact between the host and the guest is 3.699 Å. This represents the distance from C19 of the host to the centroid of the benzene ring. The angle C19-H19•••benzene was measured as 130(1)°.

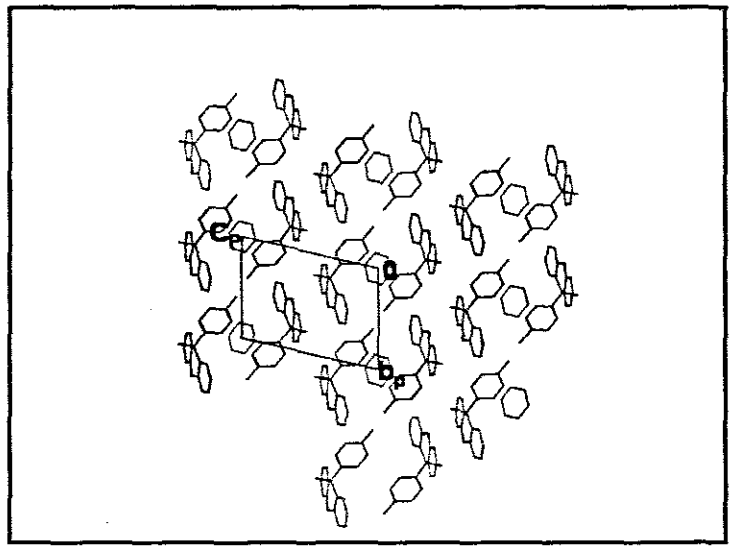

Figure 4.2 packing diagram of **A10•BENZ** along [100].

Thermal Analysis

The DSC curve shows two endotherms of which the first (T_{on}= 357.4 K) corresponds to the loss of guest and the second (T_{on}= 420.8 K) is due to the host melt.

The TG curve showed one single mass loss step. There is a good correlation between the experimental loss which is 11.9% and calculated mass loss which is 12%.

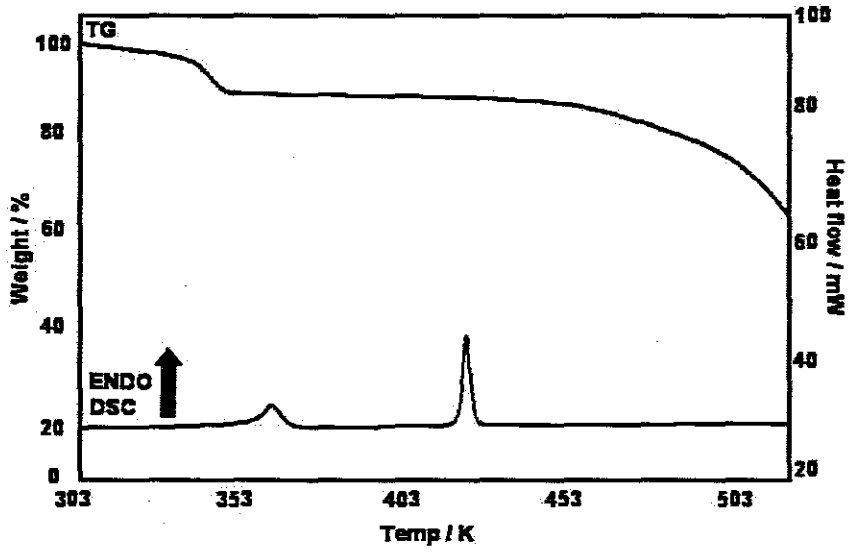

Figure 4.3 TG and DSC curve for **A10•BENZ.**

Kinetics of decomposition

Isothermal methods were used to determine the kinetics of desolvation.

Isothermal Thermogravimetry

Samples of **A10•BENZ** obtained by crushing crystals of the bulk material were analysed by performing a series of isothermal experiments over a temperature range of 323-343 K at intervals of 5K. These are shown in Figure 4.4.
The resultant α – time curves best fitted the first order reaction kinetic model, F1: -ln (1-α) = kt over the range 0 — 0.98. The resultant Arrhenius plot, Figure 4.5, revealed activation energy of 114(9) $kJmol^{-1}$.

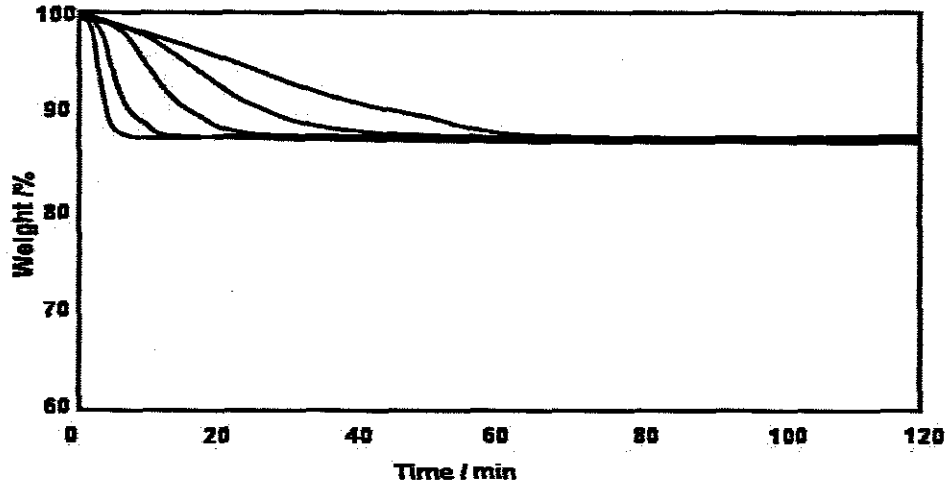

Figure 4.4 Isothermal curves of **A10•BENZ.**

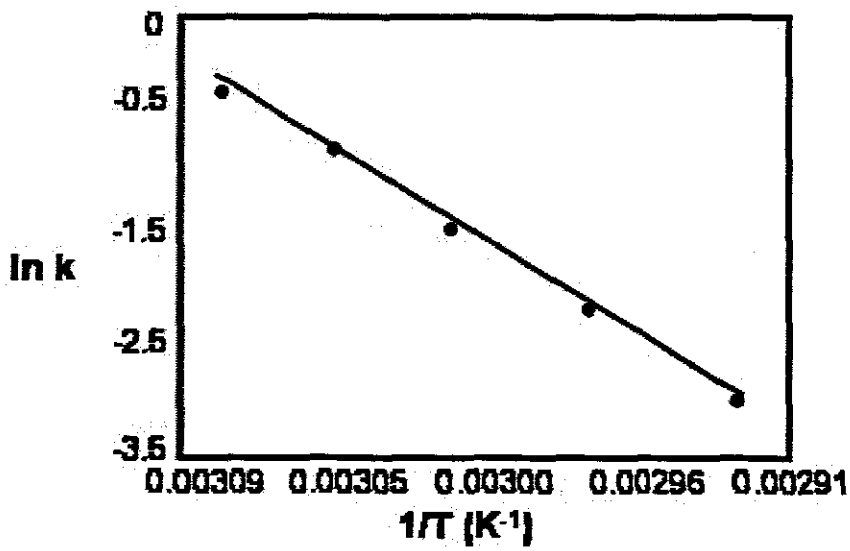

Figure 4.5 Plot of ln k versus 1/T for **A10•BENZ.**

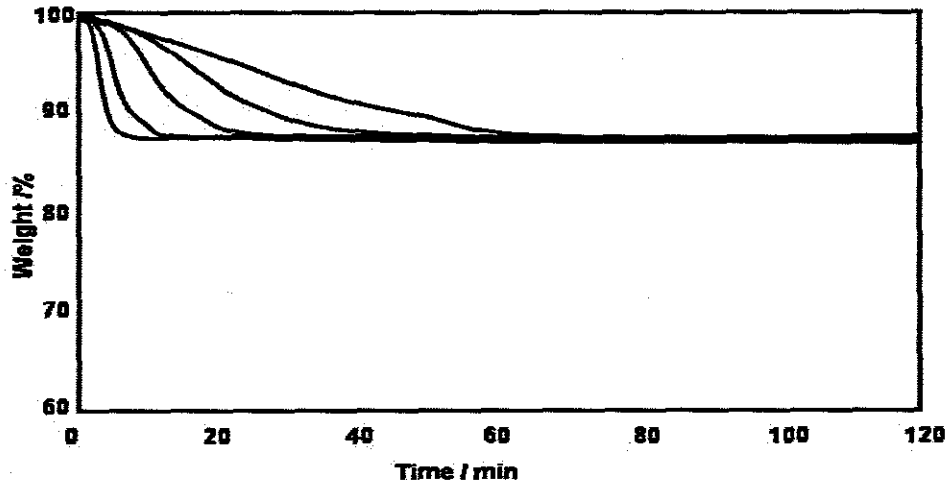

Figure 4.4 Isothermal curves of **A10•BENZ.**

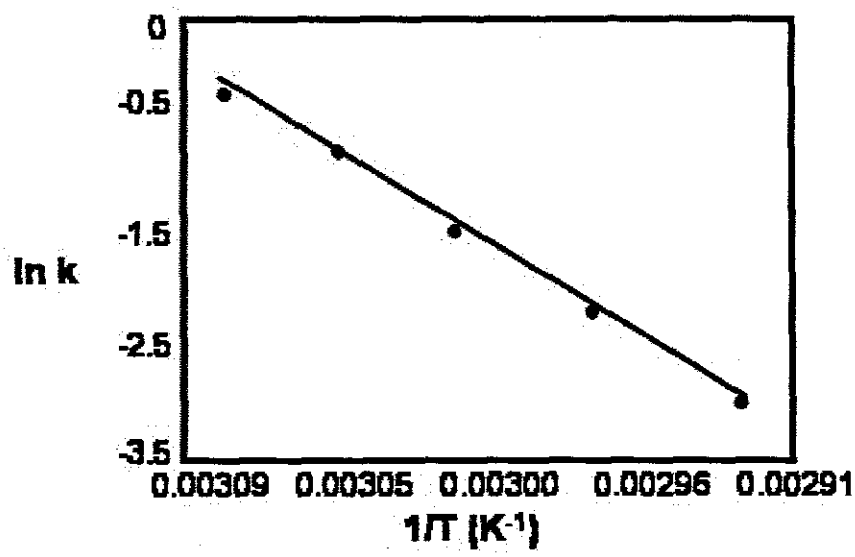

Figure 4.5 Plot of ln k versus 1/T for **A10•BENZ.**

A10•CHEX

$C_{20}H_{16}O_2 \bullet ½C_6H_{12}$
Guest: cyclohexane
Space Group: P -1
a =8.5545(17) Å α =99.93(3) °
b =9.1330(18) Å β =100.44(3) °
c= 12.068(2) Å γ =109. 42(3) °
Volume = 846.5(3) $Å^3$
Z= 2

Crystal Structure and Refinement

A host: guest ratio of 1:½ was established by TG. The crystal structures of **A10•CHEX** and **A10•BENZ** are very similar and once again the space group P -1 was assigned. Thus the host molecules were found in general positions with the cyclohexane guest on a centre of inversion (Wyckoff position *a*) in the chair conformation.

All the non-hydrogen atoms of the host and the guest were obtained by direct methods and refined anisotropically. The hydroxyl hydrogen of the host was located in the difference electron density maps and placed in geometrically calculated positions. The bond lengths and angles of the host molecule were in the expected known ranges [2].

Table 4.2 Hydrogen bonding details of **A10•CHEX.**

Donor (D)	Acceptor (A)	D•••A/Å	D—H/ Å	H•••A/Å	D-H•••A/°
O2	O1[b]	2.859(2)	0.961(1)	1.956(1)	175(2)

[b]: -x-1, -y-1, -z-1

Crystal Packing

A10•BENZ and **A10•CHEX** are isostructural with respect to the host. The host molecules form hydrogen bonded dimers with the guest molecules located in the cavities. The dimensions of the cavity were 6.06 Å x 6.77 Å x 6.89 Å. The structure is also stabilised by aromatic C-H•••π interactions between one of the guest C-H bonds and a phenyl group of the host. The C1G—H1G1•••π interaction is defined by the following: (a) the distance between C1G and the centroid of the phenyl ring defined by C7, C8, C9, C10, C11 and C12 of the host is 3.881 Å and (b) the angle C1G—H1G1•••centroid is 132(1)°.

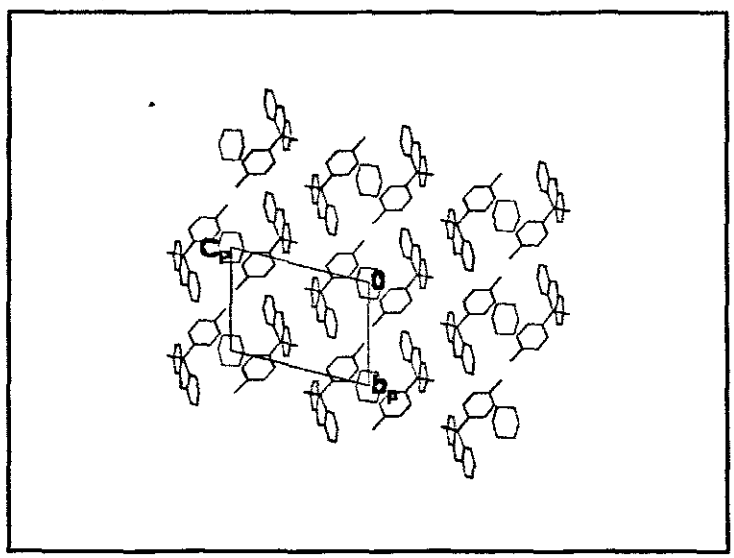

Figure 4.6 Packing diagram of **A10•CHEX** down [100].

Thermal Analysis

The TG shows a single mass loss step (calculated mass loss: 12.7%, experimental mass loss: 10.9%).

The DSC curve gave two endotherms of which the first (T_{on} = 323 K) is due to guest release and the second (T_{on} = 418, 2 K) is due to the host melt.

Crystal Packing

A10•BENZ and **A10•CHEX** are isostructural with respect to the host. The host molecules form hydrogen bonded dimers with the guest molecules located in the cavities. The dimensions of the cavity were 6.06 Å x 6.77 Å x 6.89 Å. The structure is also stabilised by aromatic C-H•••π interactions between one of the guest C-H bonds and a phenyl group of the host. The C1G—H1G1•••π interaction is defined by the following: (a) the distance between C1G and the centroid of the phenyl ring defined by C7, C8, C9, C10, C11 and C12 of the host is 3.881 Å and (b) the angle C1G—H1G1•••centroid is 132(1)°.

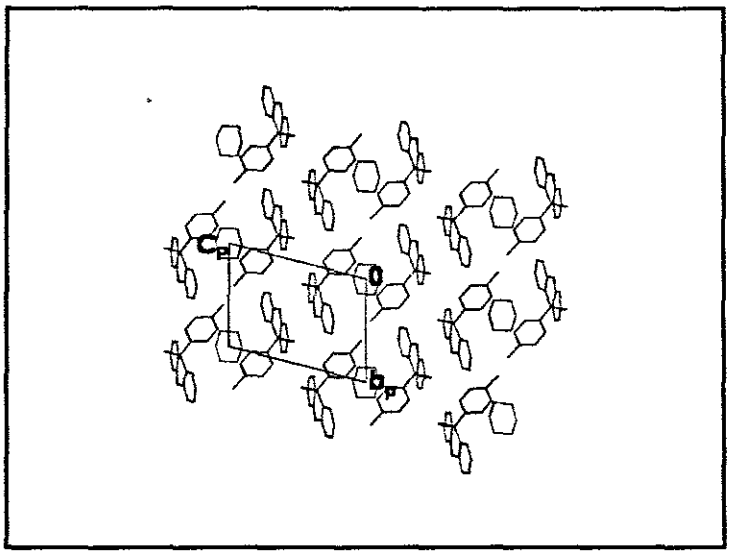

Figure 4.6 Packing diagram of **A10•CHEX** down [100].

Thermal Analysis

The TG shows a single mass loss step (calculated mass loss: 12.7%, experimental mass loss: 10.9%).

The DSC curve gave two endotherms of which the first (T_{on} = 323 K) is due to guest release and the second (T_{on} = 418, 2 K) is due to the host melt.

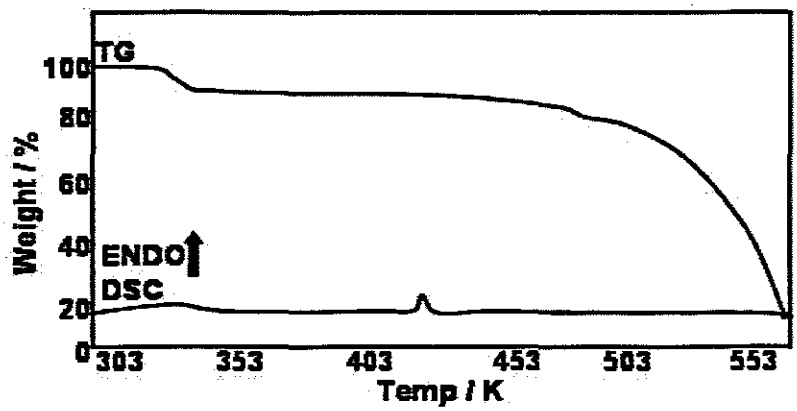

Figure 4.7 TG and DSC curves of **A10•CHEX.**

Kinetics of decomposition

Isothermal and non-isothermal methods were used to determine the kinetics of desolvation.

Isothermal Thermogravimetry

Crushed crystals of **A10•CHEX** were analysed in a series of TG runs over a temperature range of 323-338 K at intervals of 5 K. The resulting α — time curves best fitted the deceleratory first order kinetic model, F1: -ln (1-α) = kt over the range 0 to 1. The resultant Arrhenius plot, Figure 4.8, revealed an activation energy of 112(14) $kJmol^{-1}$.

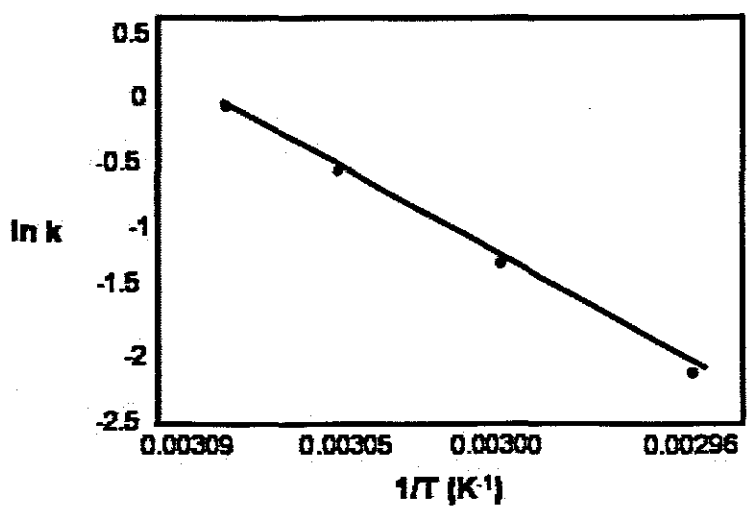

Figure 4.8 Plot of ln k versus 1/T for **A10•CHEX.**

Non-isothermal kinetics

A series of TG runs were performed over a temperature range of 303-473 K at heating rates 2, 5, 10, 15 and 20 K min^{-1}. The TG curves were analysed at percentage mass losses of 2 % to 10 % using the Flynn and Wall method [4] and converted into plots of – log ß vs. 1/T. The activation energy was calculated in the range 80-123 $kJmol^{-1}$.

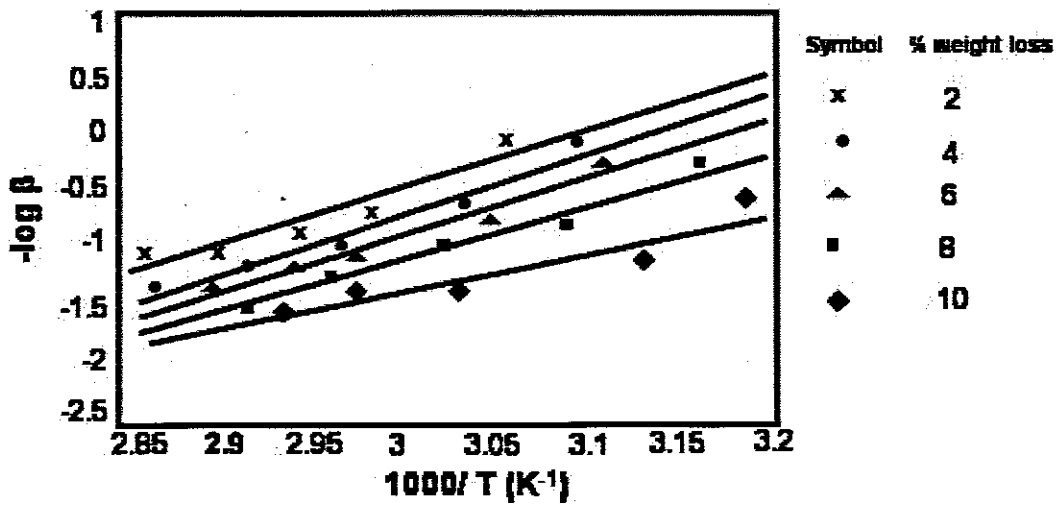

Figure 4.9 Plot of –log ß vs 1/T.

A10•CHEXANONE

$C_{20}H_{16}O_2 \bullet C_6H_{10}O$
Guest: cyclohexanone
Space Group: P -1
a =9.0694(18) Å α =85.80(3) °
b =9.5026(19) Å β =72.97(3) °
c= 12.823(3) Å γ =74.75(3) °
Volume = 1019.5(4) $Å^3$
Z= 2

Crystal Structure and Refinement

TG analysis demonstrated a host:guest ratio of 1:1. The structure was solved in the space group P -1.

The non-hydrogen atoms of the host and the guest were found in the electron density maps with both the host and guest atoms situated in general positions. Aromatic hydrogens were fixed at distances of C—H= 0.95 Å. The guest CH_2—hydrogens were fixed with C—H distances of 0.99 Å.

Table 4.3 Hydrogen bonding details of **A10•CHEXANONE.**

Donor (D)	Acceptor (A)	D•••A/Å	D—H/Å	H•••A/Å	D—H•••A/°
O2	O1[c]	2.765(2)	0.960(1)	1.829(1)	164(2)

[c]: 1-x, 1-y, -z

Crystal Packing

Each cyclohexanone molecule possesses only one oxygen atom which is capable of being a hydrogen bond acceptor. In this structure the hydroxyl hydrogen of the host forms a hydrogen bond with the oxygen of the guest. Two rows of host molecules form a bilayer parallel to [010]. The xanthene moieties

point inwards with the hydroxyl groups hydrogen bonded to the guest molecules sandwiched in-between the host bilayers. The cyclohexanone guest exhibits a chair conformation. The guest molecules lie in layers parallel to [010], with each adjacent layer antiparallel to its neighbour.

The packing of the host framework provides interconnected channels down [100] and [010]. The structure is also stabilised by a C—H•••π contact. The distance 3.901 Å was measured from C1G to the centroid of the host defined by C1, C2, C3, C4, C5 and C6. The angle C1G-H1G•••centroid is 143.24°.

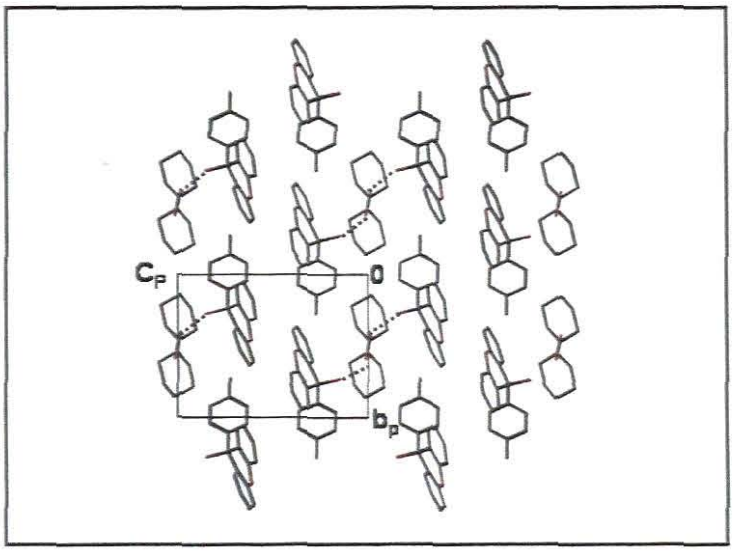

Figure 4.10 Packing diagram of **A10•CHEXANONE.**

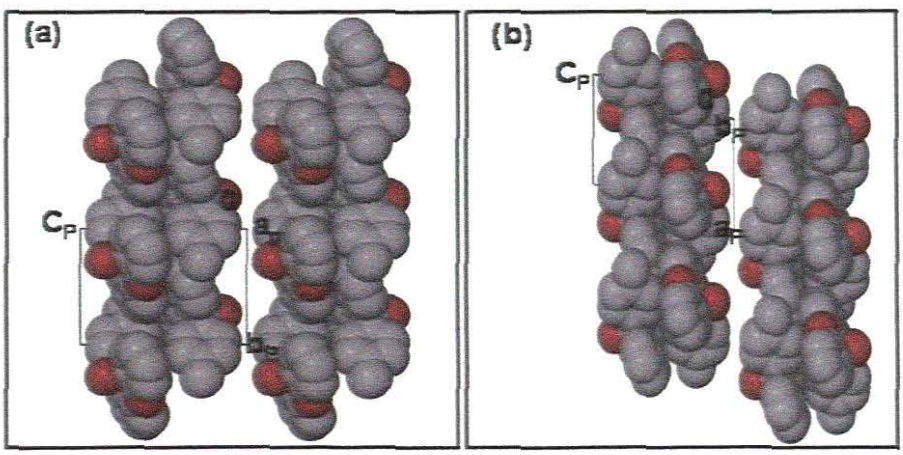

Figure 4.11 Channels of **A10•CHEXANONE** showing voids down (a) [100] and (b) [010].

Thermal Analysis

A single mass loss step was observed in the TG experiment. The experimental mass loss is 24.9% (calculated = 25.4%).

A single endotherm was observed in the DSC due to the dissolution of the host in the cyclohexanone.

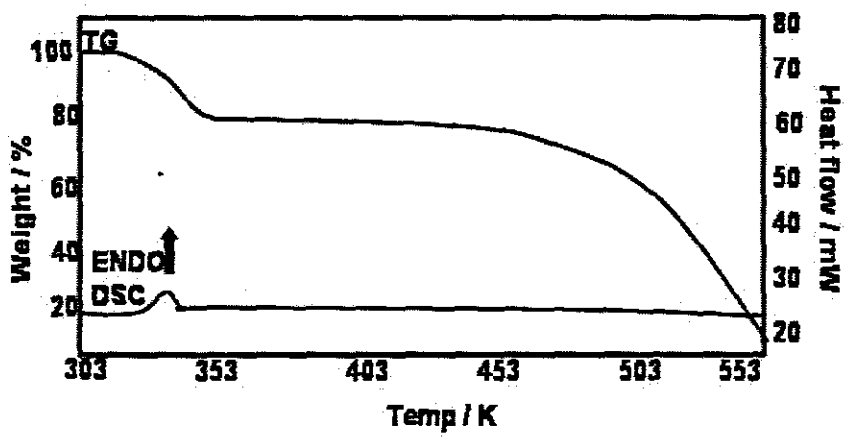

Figure 4.12 TG and DSC curve for **A10•CHEXANONE**.

Kinetics of decomposition

Non-isothermal methods were used to determine the kinetics of desolvation.

Non-isothermal kinetics

Samples of **A10•CHEXANONE** were obtained by crushing crystals of the bulk material. A series of TG runs over a temperature range of 303-473 K were performed at heating rates 1, 2, 5 and 10 K min^{-1}. The TG curves were analysed at percentage mass losses of 5% to 25 % using the Flynn and Wall method[4] and converted into plots of –log ß vs. 1/T. The activation energy was calculated in the range 80-90 $kJmol^{-1}$.

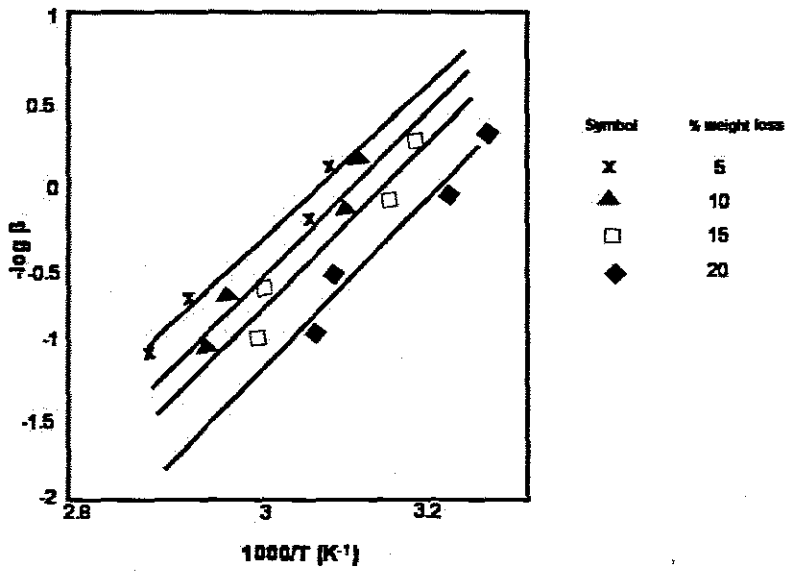

Figure 4.13 Plot of –log ß vs 1/T for **A10•CHEXANONE**.

$C_{20}H_{16}O_2 \cdot ½C_4H_8O_2$
Guest: 1, 4-dioxane
Space Group: P -1
a =8.0728(16) Å α =87.02(3) °
b =9.6524(19) Å β =85.72(3) °
c= 10.668(2) Å γ =83.97(3) °
Volume = 823.6(4) $Å^3$
Z= 2

Crystal Structure and Refinement

A host: guest ratio of 1:½ was established by TG and this was confirmed by the crystal structure. The triclinic space group P -1 was assigned. The host was found in general positions with the guest molecules situated on a centre of inversion at Wyckoff position *a*.

Again the non-hydrogen atoms of the host and guest were obtained by direct methods and refined anisotropically. The hydroxyl hydrogens were located in the difference electron density maps, and were refined isotropically. The hydroxyl hydrogens were then placed in calculated positions based on the O-H distance as a function of the O•••O distance [1].

Table 4.4 Hydrogen bonding details of **A10•DIOX**

Donor (D)	Acceptor (A)	D•••A/Å	D—H/ Å	H•••A/Å	D—H•••A/°
O2	O1G	2.868(2)	0.958(1)	1.924(1)	168(1)

Crystal Packing

The crystal packing of **A10•DIOX** is illustrated in Figure 4.14. Each dioxane molecule is hydrogen bonded to two host molecules with the dioxane in the chair conformation. By comparing the packing of **A10•DIOX**, as seen in Figure 4.14, with that of **A10•CHEX** (Figure 4.6) we notice that in the case of the packing of the dioxane compound the host hydroxyl groups are directed towards the guest whereas for the cyclohexane compound the hydroxyl hydrogens are pointed away from the guest forming dimers with adjacent host molecules. The dioxane molecules are situated in cavities which have approximate dimensions of 4.84 Å x 6.66 Å x 6.88 Å. The closest C–H•••π contact between the host and guest is 2.908 Å. This is the distance from C2G to the centroid of one of the aromatic rings of the host molecule defined by (C1, C2, C3, C4, C5 and C6). The angle C2G–H2G•••centroid is 131.55°.

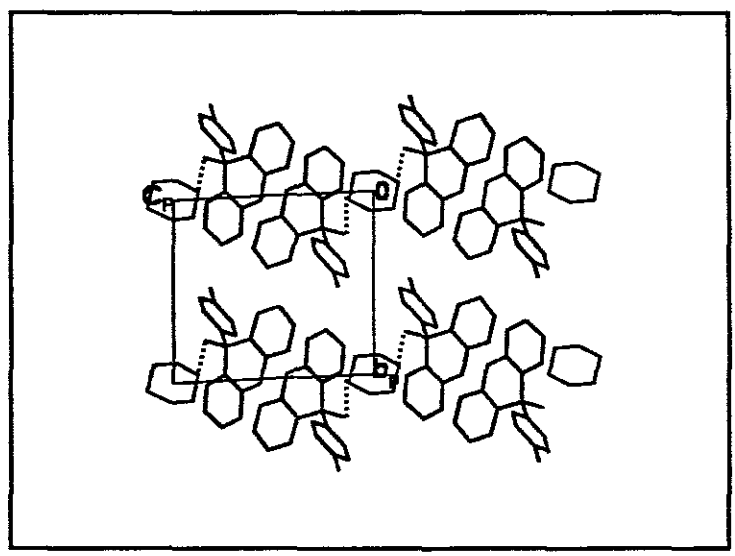

Figure 4.14 Packing diagram of **A10•DIOX** along [100].

Thermal Analysis

The DSC curve shows three endotherms of which the first (T_{on} = 327.2 K) is a very small peak compared to the other two endotherms and can be attributed to the commencement of guest release. The loss of dioxane continues at T_{on} = 384.1 K. The third endotherm (T_{on} = 399.3 K) is due to the host melt.

The results are consistent with the observations found on the melting point apparatus where the guest loss starts at 333 K and the host is completely melted at 413 K.

A single mass loss curve was observed in the TG experiment. There is a good correlation between the experimental mass loss which is 13.3 % and the calculated mass loss of 13.5 %.

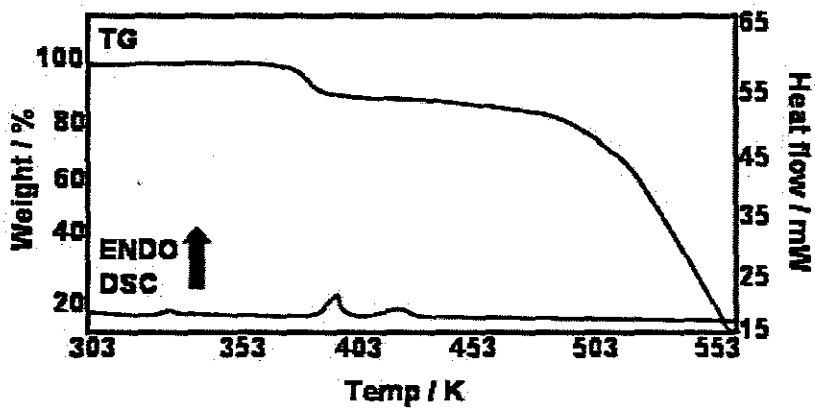

Figure 4.15 TG and DSC curve for **A10•DIOX.**

A10•DMA

$C_{20}H_{16}O_2 \cdot C_4H_9ON$
Guest: N, N-dimethylacetamide
Space Group: $P2_1/n$
a =11.135(2) Å α =90.00°
b =12.458(3) Å β =93.00(3)°
c= 14.407(3) Å γ =90.00°
Volume = 1995.8(7) $Å^3$
Z= 4

Crystal Structure and Refinement

TG analysis indicated a host:guest ratio of 1:1. The monoclinic space group $P2_1/n$ was assigned. Both the host and guest molecules were found in general positions.

The crystal structure was solved by direct methods. All the non-hydrogen atoms of the host and guest were refined anisotropically and found in the electron density maps.

Crystal Packing

The host molecules are packed in rows parallel to [010] with the ether oxygen atoms in the same direction. Each adjacent row has their ether oxygens in the opposite direction (Figure 4.17). The crystal structure is stabilized by host–guest hydrogen bonding of the form (Host)—OH•••O—(Guest) as described in Table 4.5. The shortest contact of the form (Host)—OH•••O1—(Host) was measured at 3.308 Å which is greater than the sum of the van der Waals radii and cannot be considered as a hydrogen bond. The N,N-dimethylacetamide molecules occupy zigzag channels parallel to [100] and [010].

Table 4.5 Hydrogen bonding details of **A10•DMA**.

Donor (D)	Acceptor (A)	D•••A/Å	D—H/Å	H•••A/Å	D—H•••A/°
O2	O1[d]	2.788(2)	0.960(1)	1.833(1)	173(2)

[d]: ½-x, y-½, ½-z

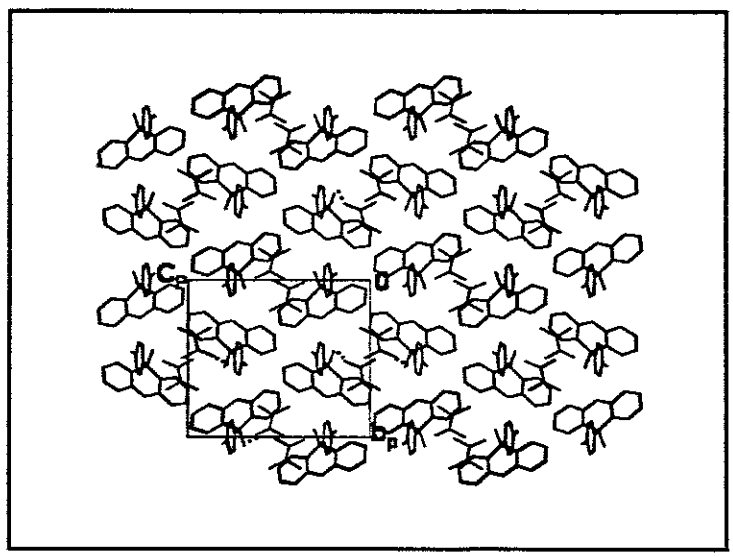

Figure 4.16 Packing diagram of **A10•DMA** down [100].

Thermal Analysis

The DSC curve shows one endotherm (T_{on} = 411.6 K). The decomposition of the crystal on the melting point apparatus verified that the host melted in the hot guest.

The TG shows a single mass loss step. The experimental mass loss is 23.1% (calculated= 23.2 %).

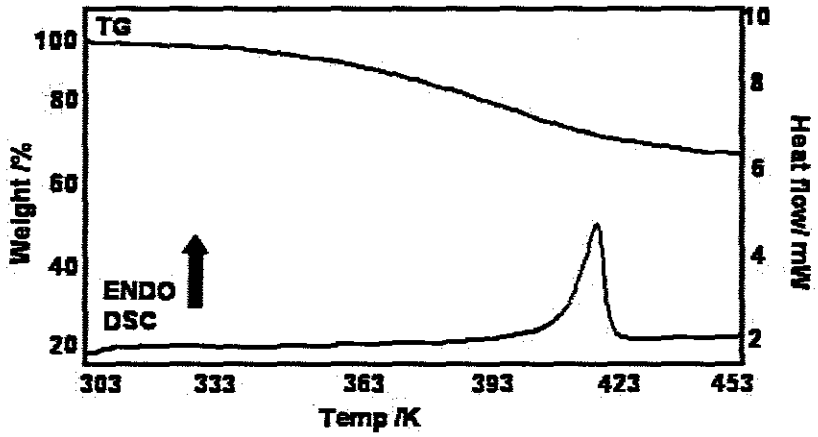

Figure 4.17 TG and DSC curve for **A10•DMA.**

A10•DMF

$C_{20}H_{16}O_2 \cdot C_3H_7ON$

Guest: N, N-dimethylformamide

Space Group: $P2_1/n$

a =12.288(3) Å α =90.00°

b =11.010(2) Å β =102.87(3) °

c= 14.758(3) Å γ =90.00°

Volume = 1946.6(7) $Å^3$

Z= 4

Crystal Structure and Refinement

The host: guest ratio of 1:1 was confirmed by TG analysis. The monoclinic space group $P2_1/n$ was assigned. The crystal structure was solved by direct methods.

The host and guest atoms were found in general positions. Again the non-hydrogen atoms of the host were found in the electron density maps and refined anisotropically. The guest atoms were solved isotropically and found to be disordered. The carbon atoms of the guest were refined and found to have the following site occupancy factors C1G: 0.7, C1GA: 0.3, C3GA: 0.3, C3G: 0.7, C2G: 0.7 and C2GA: 0.3 as shown in Figure 4.18. The resultant isotropic temperature factors were acceptable and ranged from 0.02281 Å to 0.09837 Å. The hydrogen atoms of the guest were omitted from the final refinement model.

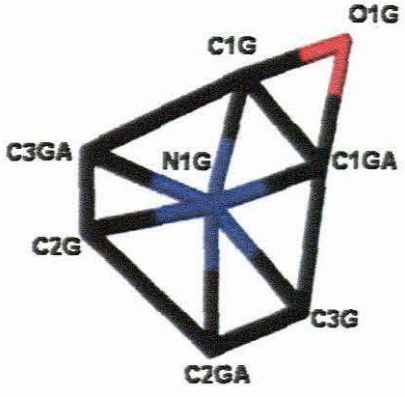

Figure 4.18 Disordered **DMF**.

Crystal Packing

Figure 4.19 illustrates the packing of **A10•DMF.** The host molecules are staggered in rows parallel to [001] with adjacent ether oxygens in an anti-parallel relationship. The guest molecules are situated in highly constricted channels parallel to [001], which are effectively cavities. Hydrogen bonding occurs between the hydroxyl hydrogen of the host and the oxygen of the guest (Table 4.6).

Table 4.6 Hydrogen bonding details of **A10•DMF**

Donor (D)	Acceptor (A)	D•••A/Å	D—H/ Å	H•••A/Å	D—H•••A/°
O2	O1G[e]	2.716(2)	0.960(1)	1.817(1)	155(2)

[e]: 1-x, 1-y, -z

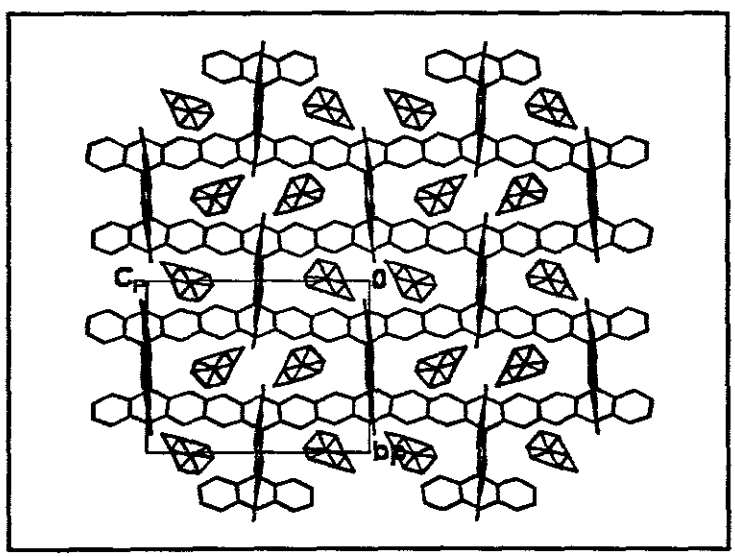

Figure 4.19 Packing diagram of **A10•DMF** down [100].

The DSC curve shows a single endotherm (T_{on} =329.9 K). The TG shows a single mass loss step (experimental mass loss = 19.7% and calculated mass loss = 20.2%).

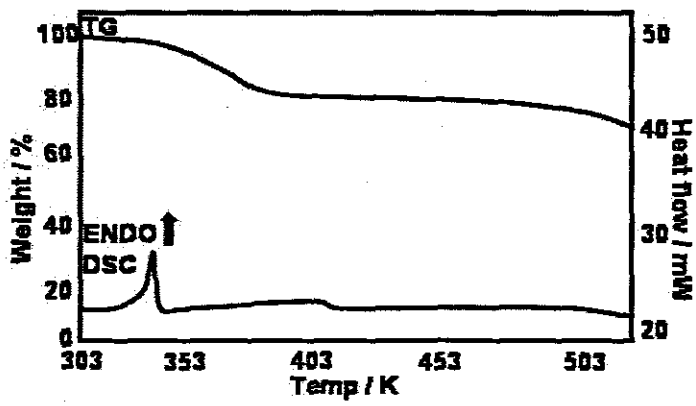

Figure 4.20 TG and DSC curves for **A10•DMF.**

Two point competition experiments were carried out between benzene and 1,4-dioxane, and N,N-dimethylacetamide and N,N-dimethylformamide. A series of 11 vials were made up with mixtures of guests in a host-guest ratio of 1:10, such that the mole fraction of one guest varied from 0 to 1. The mole fraction of a given guest included by the host versus the mole fraction of the guest in the original mother liquor was plotted. The resultant plots are shown in Figure 4.21 for benzene and 1,4-dioxane and Figure 4.22 for N,N-dimethylacetamide and N,N-dimethylformamide

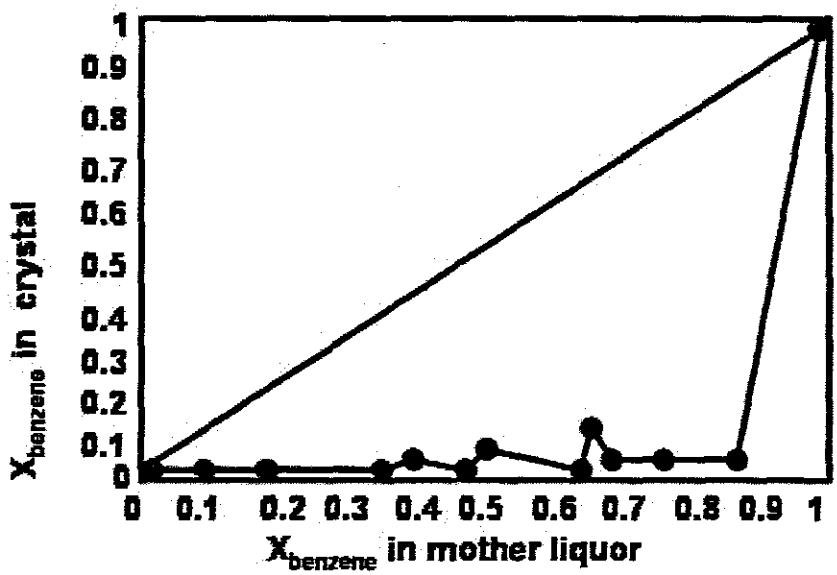

Figure 4.21 Results of competition experiments between A10 and guests benzene and 1,4-dioxane.

The results clearly indicate that **A10** preferentially includes 1,4-dioxane.

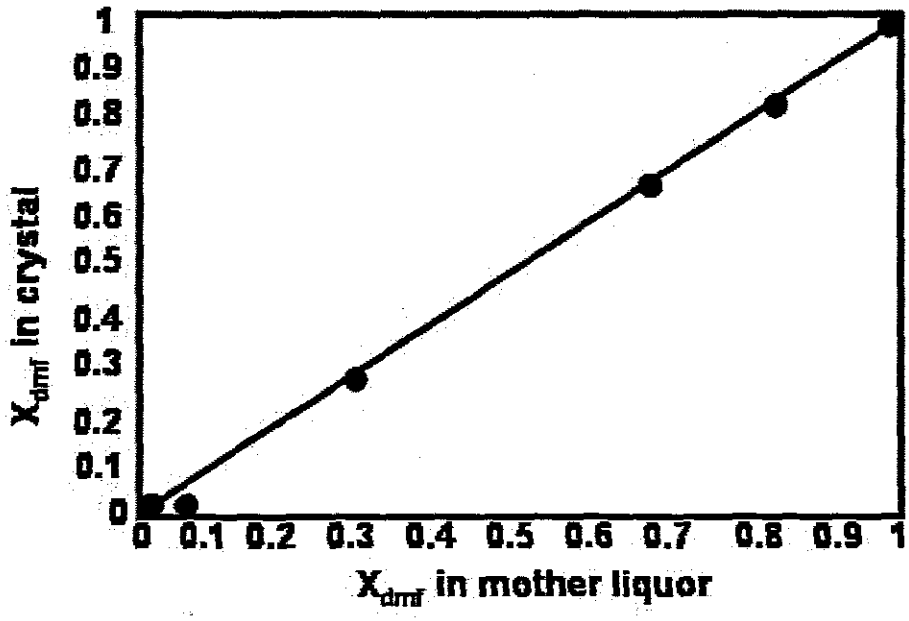

Figure 4.22 Results of competition experiments between A10 and guests N,N-dimethylacetamide and N,N-dimethylformamide.

The results show that **A10** does not differentiate between the guests N,N-dimethylacetamide and N,N-dimethylformamide.

Table 4.1 Crystal Data, experimental and refinement parameters

	A10•BENZ	**A10•CHEX**	**A10•CHEXANONE**	**A10•DIOX**	**A10•DMA**	**A10•DMF**
Compound	$C_{20}H_{16}O_2$•½C_6H_6	$C_{20}H_{16}O_2$•½C_6H_{12}	$C_{20}H_{16}O_2$•$C_6H_{10}O$	$C_{20}H_{16}O_2$•½$C_4H_8O_2$	$C_{20}H_{16}O_2$•C_4H_9ON	$C_{20}H_{16}O3$•C_3H_7ON
M_W,g.mol^{-1}	327.38	330.41	386.47	332.38	375.45	361.44
Temp/ K	173(2)	173(2)	173(2)	173(2)	173(2)	173(2)
Crystal system	P(-1)	P(-1)	P(-1)	P(-1)	$P2_1/n$	$P2_1/n$
Space Group	Triclinic	Triclinic	Triclinic	Triclinic	Monoclinic	Monoclinic
a, Å	8.4271(17)	8.5545(17)	9.0694(18)	8.0728(16)	11.135(2)	12.288(3)
b, Å	9.0895(18)	9.1330(18)	9.5026(19)	9.6524(19)	12.458(3)	11.010(2)
c, Å	11.870(2)	12.068(2)	12.823(3)	10.668(2)	14.407(3)	14.758(3)
α,°	99.86(3)	99.93(3)	85.80(3)	87.02(3)	90.00	90.00
β,°	97.55(3)	100.44(3)	72.97(3)	85.72(3)	93.00(3)	102.87(3)
γ,°	110.19(3)	109.42(3)	74.75(3)	83.97(3)	90.00	90.00
V,Å^3	822.7(3)	846.5(3)	101.95(4)	823.6(3)	1995.8(7)	1946.6(7)
Z	2	2	2	2	4	4
Absorption coefficient	0.083	0.081	0.081	0.088	0.082	0.078
F(000)	346	352	412	352	800	676
Crystal size						
Index ranges	h: ±10; k: ±-11,10; l:±14	h:±10; k:±11; l:±14	h:±11; k:±11; l:±15	h:±9; k:±11; l:±12	h:±13; k:±15; l:±17	h:±14; k:±13; l:±17
Reflections collected/ unique	3102/ 2457	3196/ 2618	3958/ 2699	2991/ 2330	3760/ 2938	3703/ 2120
Data/ restraints/ Parameters	2457/ 2/ 116	2618/ 2/ 231	2699/ 0/ 118	2330/ 0/ 227	2938/ 2/ 261	2120/ 0/ 247
Goodness-of-fit	1.049	1.060	1.120	1.186	1.096	1.114
ρ_{calc},g.cm^{-3}	1.322	1.296	1.259	1.340	1.250	1.154
Final R indices[I>2σ(I)]	R_1=0.0592 wR_2=0.1543	R1=0.0373 wR2=0.0987	R1=0.0420 wR2=0.1034	R_1=0.0529 wR_2=0.1363	R_1=0.0575 wR_2=0.1610	R1=0.0704 wR2=0.2006
R indices (all data)	R_1=0.0745 wR_2=0.1668	R_1=0.0478 wR_2=0.1050	R_1=0.0717 wR_2=0.1166	R1=0.0709 wR2=0.1485	R_1=0.0745 wR_2=0.1748	R1=0.1303 wR2=0.2434
Largest difference peak and hole,eÅ^{-3}	0.662 and -0.460	0.195 and -0.264	0.245 and -0.222	0.935 and -0.904	1.179 and -0.447	0.595 and -0.457

Discussion

All the structures were successfully solved in P -1 except for **A10•DMA** and **A10•DMF** which were solved in $P2_1/n$.

(Host)—OH•••O(Host) hydrogen bonding stabilised both the **A10•BENZ** and **A10•CHEX** structures and the packing arrangements were identical to those previously seen for the inclusion compounds formed between **A1** and the guests cyclohexane, 1,4-dioxane, benzene[6], the xylene isomers, aniline[7], naphthalene[8], anthracene and phenanthrene.

A summary of the thermal analysis data is shown in Table 4.2. In general the T_{on}/T_b values for **A10•BENZ** and **A10•CHEX** are the highest (1.012 for the benzene compound and 0.910 for the cyclohexane compound) which is indicative of their greater stability. This was also noted in Chapter 3 where the highest T_{on}/T_b values were recorded for the 1,4-dioxane and the cyclohexane compounds of **A1**.

Table 4.2 Thermal Analysis Data for A10 inclusion compounds.

ıclusion ompound	A10•BENZ	A10•CHEX	A10•CHEXANONE	A10•DIOX	A10•DMA	A10•DMF
.G ratio	1:½	1:½	1:1	1:½	1:1	1:1
G						
ılc% mass loss	11.9	12.7	25.4	13.3	23.2%	20.2
‹p% mass loss	12.0	10.9*	24.9	13.5	23.1%	19.7
SC T_{on}/K						
ıdotherm 1	357.4	322.5	325.6	327.2	411.63	329.9
ıdotherm 2	420.8	418.2		384.1		
ıdotherm 3				399.3		
(K)	353.2	354.2	428.15	374.0	439.15	426.2
$_n/T_b$	1.012	0.910	0.760	0.875	0.9373	0.774

The activation energies for the desolvation of the benzene and cyclohexanone compounds were determined as 114 $kJmol^{-1}$ and 80-90 $kJmol^{-1}$ respectively. The kinetics of desolvation for the cyclohexane compound was analysed using both isothermal and non-isothermal methods. The resultant activation energies were in good agreement; 112 $kJmol^{-1}$(isothermal kinetics) and 80-123 $kJmol^{-1}$(non-isothermal kinetics). As was expected similar values were obtained for **A10•BENZ** and **A10•CHEX** which were also higher than that obtained for **A10•CHEXANONE**. The activation energies are in the expected ranges for organic compounds of this type [6, 7].

The two point competition experiments between benzene and 1,4-dioxane indicated that the host **A10** prefers 1,4-dioxane, which is unexpected due to the greater stability of the benzene inclusion compound as indicated by the T_{on}/T_b values. A kinetic effect could explain this type of behaviour and has been reported previously[8]. For the competition between N,N-dimethylformamide and N,N-dimethylacetamide it was shown that **A10** shows no selectivity even though the T_{on}/T_b values indicate that **A10•DMA** is the more stable compound.

References:

1. I. Olovsson, P. Jönsson, *The Hydrogen Bond – Structure and Spectroscopy*, P. Schuster, G. Zundel; C. Sardify, Eds., North-Holland Publishing Company, USA, 1975.

2. International Tables for Crystallography, Vol.C, Ed., A.J.C. Wilson, Kluwer Academic Publishers, Dordrecht, 1992, pp.691.

3. L. J. Barbour, *SECTION,* a computer program for the graphical display of cross sections through a unit cell, *J.Appl.Cryst.* 1999, **32**,353.

4. J. H Flynn, L. A Wall, *J. Polym. Sci, Part B: Polym. Lett.*, 1966, **4**,323.

5. D. Braga, F. Grepioni, E. Tedesco, *Organometallics*, 1998, **17** ,2669-2672[136-137,138,199,271]

6. A. Jacobs, L. R. Nassimbeni, H. Su and B. Taljaard Org Bio.Chem., 2005, 3,1319-1322.

7. A. Jacobs, L. R. Nassimbeni, J. H. Taljaard, *CrystEngComm.* 2005, **7,** 731-734.

8. E. Curtis, L. R. Nassimbeni, H. Su and J. H. Taljaard, *Crystal Growth and Design*, 2006, 6(12), 2716-2719.

CHAPTER 5 A1 AND A10 HOST CONFORMATIONS

For host compound **A1** five different types of bonds could be distinguished excluding the ones involving hydrogen. These are shown in Figure 5.1. The conformation of the host molecule can be best described by looking at five unique torsion angles which are illustrated in Figure 5.2. The torsion angles τ_1-τ_4 describe the relative position of the xanthenol moiety to the methoxy phenyl group.

Host conformation of **A1**

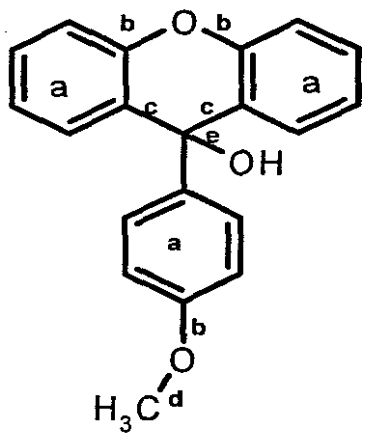

Figure 5.1 Classification of bonds for **A1**.

Table 5.1 Bond length ranges for **A1.**

Compound	a = C_{ar}—C_{ar} (Å)	b =C_{ar}—O (Å)	c= C_{ar}—C_{sp3} (Å)	d = C_{sp3}—O (Å)	e = C_{sp3}—OH (Å)
A1•CHEX	1.381(2) 1.398(2)	1.374(17) 1.393(15)	1.527(2)	1.424(16)	1.454(14)
A1•DIOX	1.378(2) 1.399(2)	1.370(18) 1.389(17)	1.528(2)	1.427(19)	1.454(14)
A1•DMF	1.376(3) 1.400(3)	1.375(3) 1.384(3)	1.528(3)	1.423(3)	1.441(2)
Reference values[1]	1.375(13) 1.391(13)	1.375(13) 1.390(15)	1.517(16) 1.539(16)	1.432(12) 1.449(12)	1.432(12) 1.449(12)

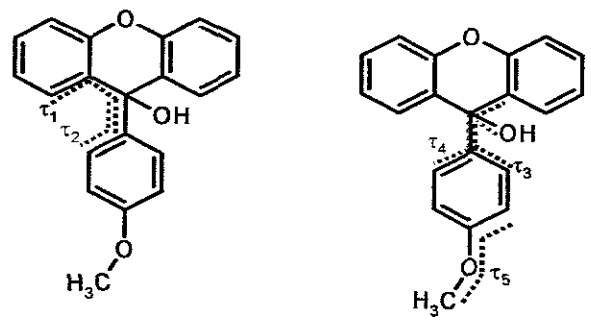

Figure 5.2 The torsion angle describing the host **A1** conformation.

Table 5.2 Torsion angles describing **A1**.

Torsion Angles	**A1•CHEX**	**A1•DIOX**	**A1•DMF**
τ_1	38.82°(15)	35.85°(19)	51.33° (17)
τ_2	61.3°(15)	59.10° (18)	58.83° (17)
τ_3	116.9°(13)	115.3° (15)	119.4° (15)
τ_4	179.8°(10)	176.8° (12)	178.1° (12)
τ_5	176.3°(12)	-179.6° (14)	11.10° (12)

A similar analysis of the bond lengths and torsion angles were completed for **A10**.

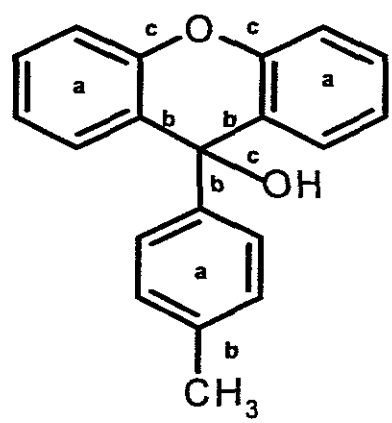

Figure 5.3 Classification of bonds for **A10.**

Table 5.3 Bond length ranges for **A10**.

Compound	**a = C_{ar}—C_{ar} (Å)**	**b = C_{ar}—C_{sp^3} (Å)**	**c = C_{sp^3}—O (Å)**
A10•BENZ	1.379(3) 1.400(3)	1.507(3) 1.525(3)	1.388(2) 1.452(2)
A10•CHEX	1.381(18) 1.396(19)	1.512(19) 1.530(18)	1.388(15) 1.450(14)
A10•CHEXANONE	1.374 (5) 1.393(4)	1.513(5) 1.529(4)	1.380(4) 1.441(4)
A10•DIOX	1.375(3) 1.436(3)	1.511(3) 1.532(3)	1.377(3) 1.446(2)
A10•DMA	1.370(4) 1.401(3)	1.511(3) 1.527(3)	1.373(3) 1 .439(2)
A10•DMF	1.365(6) 1.406(5)	1.507(6) 1.521(5)	1.378(5) 1.441(4)
Reference values[1]	1.375-1.391(13)	1.517-1.539(16)	1.380-1.442(14)

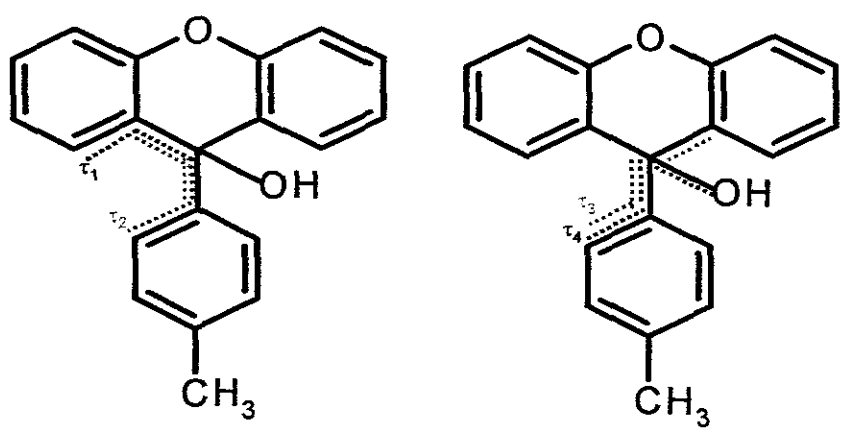

Table 5.4 The torsion angle describing the host **A10** conformation.

Torsion Angles	A10•BENZ	A10•CHEX	A10•CHEXANONE	A10•DIOX	A10•DMA	A10•DMF
τ_1	39.30°(3)	40.02° (15)	37.75° (18)	-43.10°(2)	-50.0° (2)	59.80° (3)
τ_2	63.60° (2)	62.91° (14)	64.02° (16)	-73.10°(2)	107.7° (2)	49.30° (3)
τ_3	-60.20° (2)	-60.37°(14)	-60.01° (16)	49.90°(3)	-130.6° (19)	-72.90°(3)
τ_4	-178.0° (17	-178.6°(10)	-175.3° (11)	168.2°(18)	-11.3° (2)	168.5° (2)

Reference:

1. International tables for crystallography, Vol.C,eds. A. J. C. Wilson, Kluwer Academic Publishers,Dordrecht, 1992, 691.

CHAPTER 6 CONCLUSION

Concluding Remarks

The compounds, **A1** and **A10** are both versatile hosts including a variety of small organic guest molecules. **A1** prefers to hydrogen bond with itself and form dimers which encapsulate guest molecules. The only exception being the N,N-dimethylformamide compound where for the first time for this host, host-guest hydrogen bonding was observed. **A10** also exhibits the characteristic host dimer packing motif for the benzene and cyclohexane inclusion compounds. They have proved to be rather stable with relatively high T_{on}/T_b values. Unlike **A1**, the host compound **A10** shows more diversity in its packing with various guest molecules. Host-guest hydrogen bonding was observed for the inclusion compounds of **A10** involving the guests cyclohexanone, 1,4-dioxane, N,N-dimethylformamide and N,N-dimethylacetamide.

The kinetics of desolvation for the 1, 4-dioxane and N, N-dimethylformamide inclusion compounds of **A1** gave activation energies of 133-162 kJ mol^{-1} and 143(15) kJ mol^{-1} respectively.

Similar kinetic studies were conducted for the inclusion compounds of **A10** with the guests benzene and cyclohexane. The kinetics of desolvation for **A10•BENZ** followed the first order rate law, $-\ln(1-\alpha)=kt$, and gave an activation energy of 114(9) kJ mol^{-1}. Both isothermal and non-isothermal methods were investigated for **A10•CHEX** and good agreement was obtained between these two methods. The isothermal experiments showed that the desolvation reaction proceeded via the first order rate law with activation energy of 112(14) kJ.mol^{-1} and the non-isothermal experiments gave an activation energy range of 80-123 kJ.mol^{-1}.

Competition experiments were performed for both **A1** and **A10** compounds with the following pairs of guests included by each host: benzene, and 1,4-dioxane, and N,N-dimethylformamide and N,N-dimethylacetamide.

It was found that **A1** shows no significant selectivity for 1,4-dioxane or benzene. This is expected as their structures are similar, and similar T_{on}/T_b values. The competition experiment of **A1** with the guests N,N-dimethylformamide and N,N-dimethylacetamide yielded no crystals or powders thus the competition experiments were not performed. The competition experiments for **A10** with the guests benzene and 1,4 dioxane revealed that **A10** prefers 1,4 dioxane over benzene. The guests N,N-dimethylformamide and N,N-dimethylacetamide were also included and **A10** could not differentiate between the two guests.

Appendix

Supplementary data for all crystal structures are included in the attached CD-ROM in the folder 'Appendix'.

The following files have been included for each crystal structures:

Refection data	**HKL** file
The visualisation of the structures and packing using the appropriate program X-SEED	**RES** file
Crystallographic data	**CIF** file
Tables of observed and calculated structure factors	**FCF** file
Tables of atomic co-ordination, bond lengths, bond angles, torsion angles and hydrogen bonding details.	**LST** file

All files can be viewed with a text editor such as WORDPAD or NOTEPAD.